

Penalized Projected Kernel Calibration for Computer Models*

Yan Wang [†]

Abstract. Projected kernel calibration is a newly proposed frequentist calibration method, which is asymptotic normal and semi-parametric. Its loss function is usually referred to as the *PK loss function*. In this work, we prove the uniform convergence of PK loss function and show that (1) when the sample size is large, any local minimum point and local maximum point of the L_2 loss between the true process and the computer model is a local minimum point of the PK loss function; (2) all the local minima of the PK loss function converge to the same value. These theoretical results imply that it is extremely hard for the projected kernel calibration to identify the global minimum of the L_2 loss, i.e. the optimal value of the calibration parameters. To solve this problem, a frequentist method which we term *penalized projected kernel calibration method* is suggested and analyzed in detail. We prove that the proposed method is as efficient as the projected kernel calibration method. Through an extensive set of numerical simulations, and a real-world case study, we show that the proposed calibration method can accurately estimate the calibration parameters. We also show that its performance compares favorably to other calibration methods regardless of the sample size.

Key words. Projected kernels, Calibration of computer models, Stationary points, Penalized projected kernel calibration

AMS subject classifications. 62G08, 62M30, 62M40

1. Introduction. Computer models, or simulators, are increasingly used to reproduce the behavior of complex systems in physics, engineering and human processes. Computer models usually involve model parameters that cannot be determined, or observed in the physical processes. The input values of these model parameters may significantly affect the accuracy and usefulness of the simulations' outputs. When physical observations are available, one can adjust the computer model parameters so that the computer outputs match the physical data. This stage is called the *calibration* of computer models, and the parameters are usually referred to as *calibration parameters*.

The celebrated Bayesian calibration method of Kennedy and O'Hagan [12] is one of the most widely used approaches for the calibration of computer models. We refer to [12] for more details about computer model calibration.

Let us denote the input domain of the physical experiments by Ω , which is assumed to be a convex and compact subset of \mathbf{R}^d . Let $\mathbf{X} = \{\mathbf{x}_1, \dots, \mathbf{x}_n\} \subseteq \Omega$ be the set of design points for the physical experiments and $\mathbf{Y} = (y_1, \dots, y_n)^T$ the corresponding physical responses. Throughout the paper, we denote matrices and vectors by bold symbols, with the superscript T indicating transposition. Suppose the physical experimental observation is generated by

$$(1.1) \quad y_i = \zeta(\mathbf{x}_i) + \epsilon_i,$$

*Submitted to the editors DATE.

Funding: Dr. Wang's research was supported by the National Natural Science Foundation of China (12101024), the Natural Science Foundation of Beijing Municipality (1214019).

[†]School of Statistics and Data Science, Faculty of Science, Beijing University of Technology, Beijing 100124, China (yanwang@bjut.edu.cn).

where $i = 1, \dots, n$; $\zeta(\cdot)$ is called the *true process*, which is an unknown function; ϵ_i 's are independent and identically distributed random variables with mean zero and finite variance $\sigma^2 > 0$. Suppose ϵ_i 's are sub-gaussian, that is, there exists $C_0 > 0$, such that $E[\exp(C_0|\epsilon_i|)] < \infty, i = 1, \dots, n$.

Let $y^s(\mathbf{x}, \boldsymbol{\theta})$ be the output of the deterministic computer simulator, given the control variable \mathbf{x} and the calibration parameter $\boldsymbol{\theta}$. Suppose $\boldsymbol{\theta} \in \Theta$ and assume that the parameter space Θ is a compact subset of \mathbf{R}^q . The idea of calibration is to find the values of the calibration parameters such that the computer outputs are as close as possible to the physical experimental observations.

Since computer models are usually built using assumptions and simplifications which are not exactly correct in practice, Kennedy and O'Hagan (KO thereafter) assume that the computer outputs cannot perfectly fit the physical experimental observations. That is, there is an unavoidable *model discrepancy* between the true process and the computer model. KO use the following model (named as KO's model) to take this model discrepancy into account:

$$(1.2) \quad \zeta(\cdot) = y^s(\cdot, \boldsymbol{\theta}^*) + \delta^*(\cdot),$$

where $\boldsymbol{\theta}^*$ denotes the combination of the optimal calibration parameters and δ^* is the *model discrepancy function*. The goal of calibration is to estimate $\boldsymbol{\theta}^*$. However, equation (1.2) is not enough to fully determine $\boldsymbol{\theta}^*$, because the function δ^* is also unknown.

Upon assuming that the model discrepancy function is a realization of a Gaussian Process, KO give a Bayesian estimator of the calibration parameter. Tuo and Wu [26] have shown that the estimator suggested by KO does not converge to $\boldsymbol{\theta}^*$. The optimal calibration parameters $\boldsymbol{\theta}^*$ is defined as

$$(1.3) \quad \boldsymbol{\theta}^* := \underset{\Theta}{\operatorname{argmin}} L_2(\boldsymbol{\theta}),$$

where

$$(1.4) \quad L_2(\boldsymbol{\theta}) = \int_{\Omega} (\zeta(\mathbf{x}) - y^s(\mathbf{x}, \boldsymbol{\theta}))^2 d\mathbf{x}$$

is the L_2 loss function between the true process and the computer model.

Many efforts have been made to obtain a consistent estimator of the calibration parameter. Tuo and Wu [26] have plugged the kernel ridge regression of ζ into (1.3) to get the L_2 estimator. Wong et al. [32] have proposed a least square estimator. Gu and Wang [4] have pointed out that both the approaches have limitations in their calibration and prediction performance, especially when the number of physical observations is small. To predict the true process model more accurately, Gu and Wang [4] have proposed a scaled Gaussian Process model to mimic the model discrepancy function and gave a new Bayesian calibration method based on KO's model, termed scaled Gaussian Process model calibration method. The convergence rate of the estimator given by scaled Gaussian Process model calibration method has been proven to be slower than $n^{-1/2}$ [5] at variance with the L_2 and least square calibrations. This slower convergence rate may be an issue when an efficient estimator of the calibration parameter is needed. In order to better estimate the calibration parameter, Tuo [24] have suggested a

projected kernel calibration method based on adding an orthogonality constraint (2.4) to the KO's model. Tuo has also proven the semi-parametric consistency of this estimator.

The projected kernel calibration method has been successfully applied to the calibration of the composite fuselage simulation with a small sample [30]. However, the numerical simulations reported in [4] have shown that it may get stuck in local minima or even local maxima of the L_2 loss, especially when the sample size is large.

In this work, we first verify analytically the results obtained numerically in [4], and then propose a new calibration method which is more robust with respect to the number of physical observations. The main contribution of this work may be summarized as follows:

At first, the performance of the projected kernel calibration method is explored and the results are:

- Any local minimum point and local maximum point of the L_2 loss function is a local minimum point of the projected kernel loss function (3.3);
- All the local minimum values of the projected kernel loss function converge to the same value as the sample size tends to infinity.
- The projected kernel loss function uniformly converges to a projected kernel L_2 loss function (3.12);

These results imply that it is extremely hard for the projected kernel calibration to identify the global minima of the L_2 loss function.

Second, in order to address the drawbacks of the projected kernel calibration, we put forward a penalized projected kernel calibration method. The main idea of the proposed method is to add a penalty $\|\delta^*\|_{L_2(\Omega)}$ to the projected kernel loss function. By adding this penalty, the proposed loss function avoids the problems that exist in the projected kernel loss function. That is, the local minimum points of the proposed loss function no longer contain the local maximum points of the L_2 loss function; and the local minima of the proposed loss function are different even for a sufficiently large n . We also prove that the proposed method is semi-efficient. A theoretical comparison between the proposed method and some existing calibration methods is shown in Table 1.

Table 1
Comparison of different calibration methods

Method	Abbreviation	Consistence (Y/N)	Penalty	Consistence rate (n^{-t})
KO's calibration [12, 25]	KO	N	$\ \delta^*\ _{\mathcal{N}_K(\Omega)}$	$m/(4m+d)$
L_2 calibration [26]	L_2	Y	$\ \delta^*\ _{\mathcal{N}_K(\Omega)}$	1/2
Least square calibration [32]	LS	Y	$\ \delta^*\ _{\mathcal{N}_K(\Omega)}$	1/2
Scaled Gaussian Process model calibration [4]	SGP	Y	$\ \delta^*\ _{\mathcal{N}_K(\Omega)}$ and $\ \delta^*\ _{L_2(\Omega)}$	$m/(2m+d)$
Projected kernel calibration [24]	PK	Y	$\ \delta^*\ _{\mathcal{N}_{K_{\theta^*}}(\Omega)}$	1/2
Penalized projected kernel calibration	PPK	Y	$\ \delta^*\ _{\mathcal{N}_{K_{\theta^*}}(\Omega)}$ and $\ \delta^*\ _{L_2(\Omega)}$	1/2

Remark 1: $\|\cdot\|_{L_2(\Omega)}$, $\|\cdot\|_{\mathcal{N}_K(\Omega)}$ and $\|\cdot\|_{\mathcal{N}_{K_{\theta^*}}(\Omega)}$ denote the corresponding the L_2 norm, the norm of the reproducing kernel Hilbert space generated by K and K_{θ^*} respectively.

Remark 2: Suppose the reproducing kernel Hilbert space $\mathcal{N}_K(\Omega)$ can be continuously embedded into a (fractional) Sobolev space $H^m(\Omega)$.

The paper is organized as follows. In Section 2, we give a brief review of the projected kernel calibration method. In Section 3, the performance of the projected kernel calibration method is examined theoretically and a numerical simulation is conducted to verify these theoretical assertions. In Section 4, a penalized projected kernel calibration method is introduced and its convergence properties are analyzed. Computational problems are addressed

in Section 5. The results of two numerical examples and a real-world spot welding study are presented in Section 6. Concluding remarks and further discussions are given in Section 7.

2. Review on projected kernel calibration. In this section we review the projected kernels and the projected kernel calibration.

2.1. Projected kernels. Let $K(\cdot, \cdot)$ to be a positive definite kernel function over $\Omega \times \Omega$, such as the Matérn kernel function [17, 20] with

$$(2.1) \quad K(h; \nu, \rho) = \frac{1}{\Gamma(\nu)2^{\nu-1}} \left(\frac{h}{\rho}\right)^\nu K_\nu\left(\frac{h}{\rho}\right), \nu > 0, \rho > 0,$$

where $h = \|\mathbf{x}_i - \mathbf{x}_j\|$ and $\|\cdot\|$ denotes the usual Euclidean distance; K_ν is the modified Bessel function of the second kind; ν and ρ are fixed parameters. Suppose \mathcal{G} is a finite-dimensional subspace of $L_2(\Omega)$ with $\dim \mathcal{G} = q$ and $\{e_1, \dots, e_q\}$ is a set of orthonormal basis of \mathcal{G} . For any $f \in L_2(\Omega)$, let $\mathcal{P}_{\mathcal{G}}f := \sum_{i=1}^q \langle f, e_i \rangle_{L_2(\Omega)} e_i$ be the projection of f onto \mathcal{G} and $\mathcal{P}_{\mathcal{G}}^\perp f = f - \mathcal{P}_{\mathcal{G}}f$ be the perpendicular component. Then the projected kernel of K is defined as

$$(2.2) \quad K_{\mathcal{G}} = K - \mathcal{P}_{\mathcal{G}}^{(1)}K - \mathcal{P}_{\mathcal{G}}^{(2)}K + \mathcal{P}_{\mathcal{G}}^{(1)}\mathcal{P}_{\mathcal{G}}^{(2)}K,$$

where $\mathcal{P}_{\mathcal{G}}^{(1)}, \mathcal{P}_{\mathcal{G}}^{(2)}$ are projection transformations from $L_2(\Omega \times \Omega)$ to $L_2(\Omega \times \Omega)$,

$$(2.3) \quad \begin{aligned} \mathcal{P}_{\mathcal{G}}^{(1)}K(\mathbf{x}_1, \mathbf{x}_2) &= \sum_{j=1}^q e_j(\mathbf{x}_1) \int_{\Omega} K(\mathbf{x}, \mathbf{x}_2) e_j(\mathbf{x}) d\mathbf{x}, \\ \mathcal{P}_{\mathcal{G}}^{(2)}K(\mathbf{x}_1, \mathbf{x}_2) &= \sum_{j=1}^q e_j(\mathbf{x}_2) \int_{\Omega} K(\mathbf{x}_1, \mathbf{x}) e_j(\mathbf{x}) d\mathbf{x}, \\ \mathcal{P}_{\mathcal{G}}^{(1)}\mathcal{P}_{\mathcal{G}}^{(2)}K(\mathbf{x}_1, \mathbf{x}_2) &= \sum_{j=1}^q e_j(\mathbf{x}_1) e_j(\mathbf{x}_2) \int_{\Omega} \int_{\Omega} K(\mathbf{x}, \mathbf{t}) e_j(\mathbf{t}) e_j(\mathbf{x}) dt d\mathbf{x}. \end{aligned}$$

Theorem 3.2 in [24] proves the positive definiteness of $K_{\mathcal{G}}$.

2.2. Projected kernel calibration. Because (1.3) is generally equivalent to the orthogonality constraints

$$(2.4) \quad \int_{\Omega} \frac{\partial y^s(\mathbf{x}, \boldsymbol{\theta}^*)}{\partial \theta_j} \delta^*(\mathbf{x}) d\mathbf{x} = 0,$$

for $j = 1, 2, \dots, q$. For $\boldsymbol{\theta} = (\theta_1, \dots, \theta_q) \in \Theta$, define

$$(2.5) \quad \mathcal{G}_{\boldsymbol{\theta}} = \text{span} \left\{ \frac{\partial y^s(\cdot, \boldsymbol{\theta})}{\partial \theta_1}, \frac{\partial y^s(\cdot, \boldsymbol{\theta})}{\partial \theta_2}, \dots, \frac{\partial y^s(\cdot, \boldsymbol{\theta})}{\partial \theta_q} \right\}.$$

Let $K_{\boldsymbol{\theta}} = K_{\mathcal{G}_{\boldsymbol{\theta}}}$ to be the projected kernel and $\mathcal{N}_{K_{\boldsymbol{\theta}}}(\Omega)$ the reproducing kernel Hilbert space generated by $K_{\boldsymbol{\theta}}$ [31]. Tuo [24] claims that the function space that $\delta^*(\cdot)$ belongs to should

be orthogonal to \mathcal{G}_{θ^*} . By assuming $\delta^* \in \mathcal{N}_{K_{\theta^*}}(\Omega)$, the projected kernel smoothing estimator $(\hat{\boldsymbol{\theta}}_{PK}, \hat{\delta}_{PK})$ is defined as the minimizer of

$$(2.6) \quad \min_{\boldsymbol{\theta} \in \Theta} \min_{g \in \mathcal{N}_{K_{\theta}}(\Omega)} \frac{1}{n} \sum_{i=1}^n (y_i - g(\mathbf{x}_i) - y^s(\mathbf{x}_i, \boldsymbol{\theta}))^2 + \lambda \|g\|_{\mathcal{N}_{K_{\theta}}(\Omega)}^2,$$

where λ is a tuning parameter, which can be chosen by generalized cross validation (GCV); see [11]. Following from the representer's theorem [18, 29], $\hat{\boldsymbol{\theta}}_{PK}$ can also be represented by

$$(2.7) \quad \hat{\boldsymbol{\theta}}_{PK} = \underset{\Theta}{\operatorname{argmin}} (\mathbf{Y} - \mathbf{Y}_{\theta^s})^T (\mathbf{K}_{\theta} + n\lambda \mathbf{I}_n)^{-1} (\mathbf{Y} - \mathbf{Y}_{\theta^s}).$$

where \mathbf{I}_n is the identity matrix, $\mathbf{Y}_{\theta^s} = (y^s(\mathbf{x}_1, \boldsymbol{\theta}), \dots, y^s(\mathbf{x}_n, \boldsymbol{\theta}))^T$, and $\mathbf{K}_{\theta} = [K_{\theta}(\mathbf{x}_i, \mathbf{x}_j)]_{1 \leq i, j \leq n}$. Theorem 4.3 of [24] shows that the projected kernel estimation $\hat{\boldsymbol{\theta}}_{PK}$ is asymptotically normally distributed and there does not exist a regular estimator with even smaller asymptotic variance than $\hat{\boldsymbol{\theta}}_{PK}$.

A bayesian interpretation for the projected kernel calibration is also given in [24]. Suppose $\zeta(\cdot) - y^s(\cdot, \boldsymbol{\theta})$ is a realization of Gaussian Process $GP(0, \tau^2 K_{\theta})$, where τ^2 is the variance of the covariance function and K_{θ} is the correlation function. Denote the prior distribution of $\boldsymbol{\theta}$ as $\pi(\boldsymbol{\theta})$, the posterior of $\boldsymbol{\theta}$ can be presented as

$$(2.8) \quad \pi(\boldsymbol{\theta} | \mathbf{Y}, \mathbf{Y}^s) \propto \pi(\boldsymbol{\theta}) \times \exp \left\{ -\frac{1}{2} (\mathbf{Y} - \mathbf{Y}_{\theta^s})^T (\mathbf{K}_{\theta} + n\lambda \mathbf{I}_n)^{-1} (\mathbf{Y} - \mathbf{Y}_{\theta^s}) \right\},$$

where $n\lambda = \sigma^2/\tau^2$ and an uninformative prior is used in projected kernel calibration, that is $\pi(\boldsymbol{\theta}) = 1$.

3. Performance of the projected kernel calibration. In this Section, we examine the performance of the projected kernel calibration. In subsection 3.1, we introduce the PK loss function and discuss the relationship between the local extrema of the L_2 loss function and those of the PK loss function. The uniform convergence of the PK loss function is proved in subsection 3.2, which shows that all the local minima of the PK loss function converge to a single value. In subsection 3.3, the numerical study in [4] is revisited to validate our theoretical findings.

3.1. Local minima of the PK loss function. The straightforward way to find the local minima of the PK loss function is to calculate its first and the second derivatives: the first derivative at any local minimum is zero and the Hessian matrix is positive definite. To this aim, we first rewrite (2.6) to explicit the dependence on $\boldsymbol{\theta}$.

Proposition 3.1. Define $\delta^{\theta}(\cdot) = \zeta(\cdot) - y^s(\cdot, \boldsymbol{\theta})$, $\delta_i^{\theta} = y_i - y^s(\mathbf{x}_i, \boldsymbol{\theta})$. For each $\boldsymbol{\theta} \in \Theta$, let $\hat{\delta}_{PK}^{\theta}$ to be the projected kernel smoothing estimator of δ^{θ} which is defined as

$$(3.1) \quad \hat{\delta}_{PK}^{\theta}(\mathbf{x}) = \underset{g \in \mathcal{N}_{K_{\theta}}(\Omega)}{\operatorname{argmin}} \frac{1}{n} \sum_{i=1}^n \left(\delta_i^{\theta} - g(\mathbf{x}_i) \right)^2 + \lambda \|g\|_{\mathcal{N}_{K_{\theta}}(\Omega)}^2$$

where $K_{\theta}(\mathbf{x}, \mathbf{X}) = (K_{\theta}(\mathbf{x}, \mathbf{x}_1), \dots, K_{\theta}(\mathbf{x}, \mathbf{x}_n))^T$. Then $\hat{\boldsymbol{\theta}}_{PK}$ can be written as

$$(3.2) \quad \hat{\boldsymbol{\theta}}_{PK} = \underset{\Theta}{\operatorname{argmin}} L_{PK}(\boldsymbol{\theta}),$$

where

$$(3.3) \quad L_{PK}(\boldsymbol{\theta}) = \frac{1}{n} \sum_{i=1}^n \left(\delta_i^\theta - \hat{\delta}_{PK}^\theta(\mathbf{x}_i) \right)^2 + \lambda \|\hat{\delta}_{PK}^\theta\|_{\mathcal{N}_{K_\theta}(\Omega)}^2.$$

The loss function (3.3) is referred to as the projected kernel loss function (abbreviated as PK loss function).

From (3.3), we can see that the derivative of the PK loss function depends on the derivatives of $\hat{\delta}_{PK}^\theta$ and $\|\hat{\delta}_{PK}^\theta\|_{\mathcal{N}_{K_\theta}(\Omega)}^2$ with respect to $\boldsymbol{\theta}$. Since $\hat{\delta}_{PK}^\theta$ belongs to the functional space $\mathcal{N}_{K_\theta}(\Omega)$, which itself depends on $\boldsymbol{\theta}$, it is difficult to evaluate the derivatives of $\hat{\delta}_{PK}^\theta$ and $\|\hat{\delta}_{PK}^\theta\|_{\mathcal{N}_{K_\theta}(\Omega)}^2$ with respect to $\boldsymbol{\theta}$ directly. To solve this problem, we look for a function $\hat{\delta}^\theta$ in the functional space $\mathcal{N}_K(\Omega)$ such that $\hat{\delta}_{PK}^\theta = \mathcal{P}_{\mathcal{G}_\theta}^\perp \hat{\delta}^\theta$. Here $\mathcal{N}_K(\Omega)$ denotes the reproducing kernel Hilbert space generated by K . It is clear that $\mathcal{N}_K(\Omega)$ is not dependent on $\boldsymbol{\theta}$. Proposition 3.2 shows the result.

Proposition 3.2. Define the loss function l_θ as

$$(3.4) \quad l_\theta(g_0) = \frac{1}{n} \sum_{i=1}^n \left(\delta_i^\theta - \mathcal{P}_{\mathcal{G}_\theta} g_0(\mathbf{x}_i) \right)^2 + \frac{1}{n} \sum_{i=1}^n \left(\delta_i^\theta - \mathcal{P}_{\mathcal{G}_\theta}^\perp g_0(\mathbf{x}_i) \right)^2 + \lambda \|\mathcal{P}_{\mathcal{G}_\theta}^\perp g_0\|_{\mathcal{N}_{K_\theta}(\Omega)}^2,$$

where $g_0 \in \mathcal{N}_K(\Omega)$. Let $\hat{\delta}^\theta = \operatorname{argmin}_{g_0 \in \mathcal{N}_K(\Omega)} l_\theta(g_0)$. Assuming \mathcal{G}_θ (2.5) is a subspace of $\mathcal{N}_K(\Omega)$, then there exists $\hat{\delta}_{PK}^\theta$, which is defined in (3.1), such that

$$\hat{\delta}_{PK}^\theta = \mathcal{P}_{\mathcal{G}_\theta}^\perp \hat{\delta}^\theta = \hat{\delta}^\theta - \mathcal{P}_{\mathcal{G}_\theta} \hat{\delta}^\theta.$$

Remark 3.3. From Theorem 3.3 in [24], if $\mathcal{G}_\theta \subset \mathcal{N}_K(\Omega)$, there exists $\mathcal{N}_{K_\theta}(\Omega) \subset \mathcal{N}_K(\Omega)$. Using this fact, one may easily prove that $\hat{\delta}_{PK}^\theta$ (3.1) is a minimizer of the loss function l_θ in $\mathcal{N}_{K_\theta}(\Omega)$.

According to Proposition 3.2, the calculation of the derivatives of $\hat{\delta}_{PK}^\theta$ is transformed into the calculation of the derivatives of $\hat{\delta}^\theta$ and $\mathcal{P}_{\mathcal{G}_\theta} \hat{\delta}^\theta$ on $\boldsymbol{\theta}$. To establish the asymptotic behavior of the derivatives of the PK loss function on $\boldsymbol{\theta}$, we first analyze how accurately $\hat{\delta}^\theta$ may approximate δ^θ in a uniform sense.

Proposition 3.4. Define the empirical norm of $g_0 \in \mathcal{N}_{K_\theta}(\Omega)$ as $\|g_0\|_n^2 = \frac{1}{n} \sum_{i=1}^n g_0^2(\mathbf{x}_i)$. Then under the following hypotheses

- A1. x_i 's are independent random samples from the uniform distribution over Ω .
- A2. $\mathcal{N}_K(\Omega)$ can be continuously embedded into the (fractional) Sobolev space $H^m(\Omega)$ with $m > d/2$.
- A3. It holds that

$$\sup_{\boldsymbol{\theta} \in \Theta, j=1,2,\dots,q} \left\{ \left\| \frac{\partial y^s(\cdot, \boldsymbol{\theta})}{\partial \theta_j} \right\|_{\mathcal{N}_K(\Omega)} / \left\| \frac{\partial y^s(\cdot, \boldsymbol{\theta})}{\partial \theta_j} \right\|_{L_2(\Omega)} \right\} < \infty,$$

$$\sup_{\boldsymbol{\theta} \in \Theta, j=1,2,\dots,q} \left\{ \left\| \frac{\partial y^s(\cdot, \boldsymbol{\theta})}{\partial \theta_j} \right\|_{L_2(\Omega)} \right\} < \infty,$$

and

$$\sup_{\boldsymbol{\theta} \in \Theta} \|y^s(\cdot, \boldsymbol{\theta})\|_{\mathcal{N}_K(\Omega)} < \infty.$$

A4. Define the matrix \mathbf{E}_θ as

$$(3.5) \quad \mathbf{E}_\theta = \left[\int \frac{\partial y^s(\mathbf{x}, \boldsymbol{\theta})}{\partial \theta_i} \frac{\partial y^s(\mathbf{x}, \boldsymbol{\theta})}{\partial \theta_j} d\mathbf{x} \right]_{1 \leq i, j \leq q}.$$

Assume $\inf_{\boldsymbol{\theta} \in \Theta} \lambda_{\min}(\mathbf{E}_\theta) > 0$, where $\lambda_{\min}(\mathbf{E}_\theta)$ is the minimum eigenvalue of \mathbf{E}_θ .

We have that if $\lambda \sim n^{-\frac{2m}{2m+d}}$,

$$(3.6) \quad \begin{aligned} \sup_{\boldsymbol{\theta} \in \Theta} \left\| \delta^\theta - \hat{\delta}^\theta \right\|_{L_2(\Omega)} &= O_p(n^{-\frac{m}{2m+d}}), \\ \sup_{\boldsymbol{\theta} \in \Theta} \left\| \hat{\delta}_{PK}^\theta \right\|_{\mathcal{N}_{K_\theta}(\Omega)} &= O_p(1). \end{aligned}$$

Remark 3.5. Condition A2 can be met easily if K is chosen to be a Matérn kernel (2.1). By the Corollary 1 of [27], the reproducing kernel Hilbert space generated by the Matérn kernel is equal to the (fractional) Sobolev space $H^{\nu+d/2}(\Omega)$, with equivalent norms.

Corollary 3.6. Under the conditions of Proposition 3.4, we have that if $\lambda \sim n^{-\frac{2m}{2m+d}}$, then

$$\sup_{\boldsymbol{\theta} \in \Theta} \left\| \mathcal{P}_{\mathcal{G}_\theta}^\perp \delta^\theta - \hat{\delta}_{PK}^\theta \right\|_{L_2(\Omega)} = O_p(n^{-\frac{m}{2m+d}}).$$

It is worth noticing that Proposition 3.4 is different from Theorem 4.1 in [24]. Let $\hat{\zeta}_{PK}(\cdot) = \hat{\delta}_{PK}^{\hat{\theta}}(\cdot) + y^s(\cdot, \hat{\boldsymbol{\theta}}_{PK})$ be the predictor given by the projected kernel calibration. Theorem 4.1 in [24] shows that, under certain conditions, there is $\|\hat{\zeta}_{PK} - \zeta\|_{L_2(\Omega)} = O_p(n^{-\frac{m}{2m+d}})$. It is an immediate consequence of the combination of Corollary 3.6 and the asymptotic normal of the projected kernel calibration. Let us briefly explain the reasons.

By the triangle inequality, $\|\hat{\zeta}_{PK} - \zeta\|_{L_2(\Omega)}$ can be bounded from above

$$\left\| \hat{\delta}_{PK}^{\hat{\theta}^*} - \delta^* \right\|_{L_2(\Omega)} + \left\{ \left\| \hat{\delta}_{PK}^{\hat{\theta}} - \hat{\delta}_{PK}^{\hat{\theta}^*} \right\|_{L_2(\Omega)} + \left\| y^s(\cdot, \hat{\boldsymbol{\theta}}_{PK}) - y^s(\cdot, \boldsymbol{\theta}^*) \right\|_{L_2(\Omega)} \right\}.$$

Next, we bound these two terms separately. Because $\delta^* = \delta^{\theta^*} \in \mathcal{G}_{\theta^*}^\perp$, from Corollary 3.6, the first term is equal to $O_p(n^{-\frac{m}{2m+d}})$. It follows from Taylor's theorem, Cauchy-Schwarz inequality, and the asymptotic normal of the projected kernel calibration that, the second term is equal to $O_p(n^{-1/2})$. The desired result of Theorem 4.1 in [24] can be easily obtained by the summation of these two bounds.

Theorem 3.7. Under the conditions of Proposition 3.4, we have that

$$(3.7) \quad \sup_{\boldsymbol{\theta} \in \Theta} \left| \frac{\partial L_{PK}(\boldsymbol{\theta})}{\partial \theta_j} - \frac{\partial \mathbf{a}_\theta^T \mathbf{E}_\theta^{-1} \mathbf{a}_\theta}{\partial \theta_j} \right| = O_p(n^{-\frac{m}{2m+d}}), j = 1, 2, \dots, q,$$

where $\mathbf{a}_\theta^T = \langle \delta^\theta(\cdot), \frac{\partial y^s(\cdot, \boldsymbol{\theta})}{\partial \theta} \rangle_{L_2(\Omega)}$.

Let $\boldsymbol{\theta}^s$ to be a stationary point of the L_2 loss function, then the Hessian matrix of $L_{PK}(\boldsymbol{\theta})$ at $\boldsymbol{\theta}^s$, denotes as $\mathbf{H}_{PK}(\boldsymbol{\theta}^s)$ may be written as

$$(3.8) \quad \mathbf{H}_{PK}(\boldsymbol{\theta}^s) = 2 \frac{\partial \mathbf{a}_{\boldsymbol{\theta}^s}^T}{\partial \boldsymbol{\theta}} \mathbf{E}_{\boldsymbol{\theta}^s}^{-1} \frac{\partial \mathbf{a}_{\boldsymbol{\theta}^s}^T}{\partial \boldsymbol{\theta}} + O_p(n^{-\frac{m}{2m+d}}).$$

Corollary 3.8. Under the condition of Proposition 3.4, we have that if $\boldsymbol{\theta}^s$ is a local maxima or local minima of the L_2 loss function, then $\lim_{n \rightarrow \infty} \frac{\partial L_{PK}(\boldsymbol{\theta})}{\partial \boldsymbol{\theta}}|_{\boldsymbol{\theta}^s} = \mathbf{0}$, i.e. $\boldsymbol{\theta}^s$ is a stationary point of the PK loss function.

Corollary 3.8 is an immediate consequence of (3.7), following from the vanishing of the first derivative of $L_2(\boldsymbol{\theta})$ at $\boldsymbol{\theta}^s$ is zero, which itself is equivalent to $\mathbf{a}_{\boldsymbol{\theta}^s} = \mathbf{0}$. To check whether $\boldsymbol{\theta}^s$ is a local maximum or a local minimum of the PK loss function, let us study the sign of the Hessian matrix $\mathbf{H}_{PK}(\boldsymbol{\theta}^s)$. Since $\mathbf{E}_{\boldsymbol{\theta}^s}^{-1}$ is a positive definite matrix, then the matrix $\frac{\partial \mathbf{a}_{\boldsymbol{\theta}^s}^T}{\partial \boldsymbol{\theta}} \mathbf{E}_{\boldsymbol{\theta}^s}^{-1} \frac{\partial \mathbf{a}_{\boldsymbol{\theta}^s}^T}{\partial \boldsymbol{\theta}}$ is semi-positive definite. When the sample size n tends to infinity, we can easily prove the following corollary.

Corollary 3.9. Under the condition of Proposition 3.4, we have that if $\boldsymbol{\theta}^s$ is a local maxima or local minima of the L_2 loss function, then the Hessian matrix of the PK loss at $\boldsymbol{\theta}^s$ is positive definite.

Corollary 3.9 shows that the local optimal points of the L_2 loss function are local minima of the PK loss function. Specifically, suppose that the L_2 loss function has l local optima, denoted as $\{\boldsymbol{\theta}_1^s, \dots, \boldsymbol{\theta}_l^s\}$. If $l = 1$, then $\boldsymbol{\theta}_1^s$ is the global minimum of L_{PK} . If $l \geq 2$, then $\boldsymbol{\theta}_1^s, \dots, \boldsymbol{\theta}_l^s$ are local minima of L_{PK} .

3.2. Convergence of the PK loss function. From Theorem 10.7 in [2], we have that Theorem 3.7 alone does not indicate uniform convergence of the PK loss function. Another necessary condition is that the PK loss function converges at at least one point. Based on the definition of $L_{PK}(\boldsymbol{\theta})$ (3.3),

$$(3.9) \quad \begin{aligned} L_{PK}(\boldsymbol{\theta}^*) &= \frac{1}{n} \sum_{i=1}^n \left(\delta^*(\mathbf{x}_i) - \hat{\delta}_{PK}^{\boldsymbol{\theta}^*}(\mathbf{x}_i) \right)^2 + \frac{2}{n} \sum_{i=1}^n \epsilon_i \left(\delta^*(\mathbf{x}_i) - \hat{\delta}_{PK}^{\boldsymbol{\theta}^*}(\mathbf{x}_i) \right) + \\ &\quad \frac{1}{n} \sum_{i=1}^n \epsilon_i^2 + \lambda \|\hat{\delta}_{PK}^{\boldsymbol{\theta}^*}\|_{\mathcal{N}_{K_{\boldsymbol{\theta}^*}}(\Omega)}^2. \end{aligned}$$

Combining (3.9), (A.7), (A.10) and Proposition 3.4, we have that if $\lambda \sim n^{-\frac{2m}{2m+d}}$, there is $L_{PK}(\boldsymbol{\theta}^*) = \frac{1}{n} \sum_{i=1}^n \epsilon_i^2 + O_p(n^{-\frac{2m}{2m+d}}) < \infty$. Let us now denote $C_1 = \lim_{n \rightarrow \infty} L_{PK}(\boldsymbol{\theta}^*) = \sigma^2 < \infty$. The uniform convergence of $\frac{\partial L_{PK}(\boldsymbol{\theta})}{\partial \theta_j}$, $j = 1, \dots, q$ and the convergence of $L_{PK}(\boldsymbol{\theta}^*)$ guarantee the uniform convergence of $L_{PK}(\boldsymbol{\theta})$, that is

$$(3.10) \quad \lim_{n \rightarrow \infty} \sup_{\boldsymbol{\theta} \in \Theta} |L_{PK}(\boldsymbol{\theta}) - \mathbf{a}_{\boldsymbol{\theta}}^T \mathbf{E}_{\boldsymbol{\theta}}^{-1} \mathbf{a}_{\boldsymbol{\theta}} - C_1| = 0.$$

Since $\mathcal{P}_{\mathcal{G}_{\boldsymbol{\theta}}} \delta^{\boldsymbol{\theta}} = \mathbf{a}_{\boldsymbol{\theta}}^T \mathbf{E}_{\boldsymbol{\theta}}^{-1} \frac{\partial y^s(\cdot; \boldsymbol{\theta})}{\partial \boldsymbol{\theta}^T}$, it follows from basic linear algebra that

$$(3.11) \quad \mathbf{a}_{\boldsymbol{\theta}}^T \mathbf{E}_{\boldsymbol{\theta}}^{-1} \mathbf{a}_{\boldsymbol{\theta}} = \langle \delta^{\boldsymbol{\theta}}, \mathcal{P}_{\mathcal{G}_{\boldsymbol{\theta}}} \delta^{\boldsymbol{\theta}} \rangle_{L_2(\Omega)} = \|\mathcal{P}_{\mathcal{G}_{\boldsymbol{\theta}}} \delta^{\boldsymbol{\theta}}\|_{L_2(\Omega)}^2.$$

Upon combining (3.10) and (3.11), Theorem 3.10 shows the uniform convergence of $L_{PK}(\boldsymbol{\theta})$.

Theorem 3.10. *Under the condition of Proposition 3.4, we have that*

$$(3.12) \quad \lim_{n \rightarrow \infty} \sup_{\boldsymbol{\theta} \in \Theta} \left| L_{PK}(\boldsymbol{\theta}) - \|\mathcal{P}_{\mathcal{G}_\theta} \delta^\theta\|_{L_2(\Omega)}^2 - C_1 \right| = 0.$$

$\|\mathcal{P}_{\mathcal{G}_\theta} \delta^\theta\|_{L_2(\Omega)}^2 + C_1$ is termed the projected kernel L_2 loss function (PKL2 loss function).

Since δ_i^s is orthogonal to $\mathcal{G}_{\theta_i^s}$, Theorem 3.10 shows that $\lim_{n \rightarrow \infty} L_{PK}(\boldsymbol{\theta}_i^s) = C_1$ for any $i = 1, \dots, l$. That is, all the local minima of the PK loss functions approach the same value. This implies that the projected kernel calibration method may easily get stuck in local minima or even local maxima of the L_2 loss function.

3.3. Revisit the Example 2 in [4]. To validate our theoretical assertions, the numerical study in [4] is revisited in this subsection. Example 2 in [4] shows that L_{PK} tends to have more local optimal points than the L_2 loss function. In this example, the smoothness of discrepancy function is infinite, whereas [4] choose a Matérn kernel function (2.1) with $\nu = 1/2$ to estimate the discrepancy function. To avoid the effect of inaccuracy of the correlation function, we make some modifications to this example.

Suppose the true process is

$$\zeta(x) = x \cos(3x/2) + x, x \in [0, 5].$$

The computer model is

$$y^s(x, \theta) = \sin(\theta x) + \exp(-2|x|), \theta \in [0, 3].$$

By the definition of θ^* (1.3), we have that $\theta^* = 0.371$. Because the smoothness of $\zeta(\cdot) - y^s(\cdot, \theta)$ depends on the smoothness of $\exp(-2|x|)$, we have that the discrepancy function is in the reproducing kernel Hilbert space generated by the Matérn kernel function $K(h; \frac{1}{2}, \frac{1}{2})$, which is equal to the Sobolev space $H^1(\Omega)$.

Let $\{x_1, x_2, \dots, x_n\}$ be the set of the design points, where $x_i = -5 + \frac{10(i-1)}{n-1}$, $i = 1, 2, \dots, n$ and $n = 100$ is the sample size. Suppose the observation error ϵ_i 's are mutually independent and follow from $N(0, 0.2^2)$. By Proposition 3.4, set the tuning parameter $\lambda = \beta n^{-\frac{2}{3}}$ and β is chosen by 10-fold cross validation method [11]. With the help of *caret* Package [13] in R, we have that $\beta = 0.00138$. To illustrate the performance of the projected kernel calibration more clearly, we scale these two loss function to $[0, 1]$ respectively. The scaled value of loss function L is defined as

$$(3.13) \quad \frac{L(\boldsymbol{\theta}) - \min_{\Theta} L(\boldsymbol{\theta})}{\max_{\Theta} L(\boldsymbol{\theta}) - \min_{\Theta} L(\boldsymbol{\theta})}.$$

Figure 1 shows the comparison between the PK loss function and the L_2 loss function when the sample size $n = 100$. The scaled L_2 loss over $\theta \in [0, 3]$ is shown in the black solid line, which contains a global minimum at 0.371, a local minimum at 1.855, two local maxima at 1.122 and 2.545 respectively. The PK loss function (dashed line) has a global minimum at 0.371, and three local minima at the three local optimal points of the L_2 loss function.

Figure 2 compares the PK loss function with the PKL2 loss function when the sample size $n = 100$. We can see that the red dashed line is completely coincident with the green real line. It indicates the PK loss function converges to the PKL2 loss function when the sample size is 100.

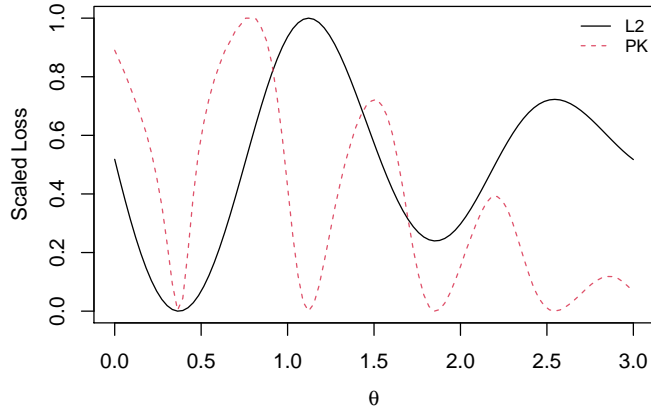


Figure 1. PK loss function (red dashed line) v.s. L_2 loss function (black real line).

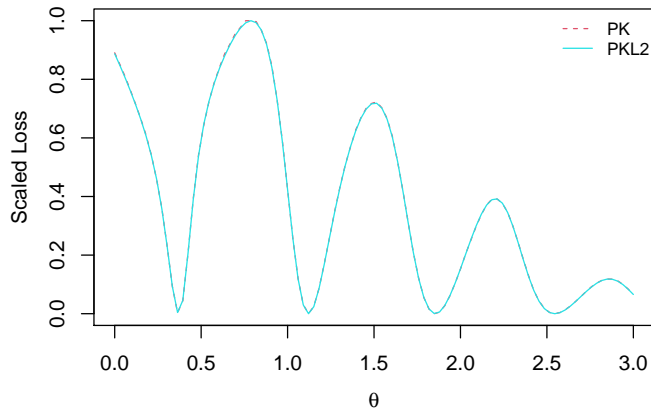


Figure 2. PK loss function (red dashed line) v.s. PKL2 loss function (blue real line).

4. Penalized projected kernel calibration. The uniform convergence of the PK loss function leads to the failure of any kind of global optimization. To overcome the problem, and inspired by [4], we rescale the L_2 norm of the discrepancy function, and introduce a penalized projected kernel calibration method.

4.1. Methodology. We define the penalized projected kernel estimator of θ as

$$(4.1) \quad \hat{\theta}_{PPK} = \underset{\Theta}{\operatorname{argmin}} \left\{ L_{PK}(\theta) + \eta \|\delta^\theta\|_{L_2(\Omega)}^2 \right\}.$$

As δ^θ is unknown, a natural choice is to replace δ^θ by its estimator. Since Proposition 3.4 guarantees that a proper choice to estimate δ^* is $\hat{\delta}_{PK}^{\theta^*}$, we propose to evaluate $\hat{\boldsymbol{\theta}}_{PPK}$ by minimizing the following loss function

$$(4.2) \quad L_{PPK}(\boldsymbol{\theta}) = L_{PK}(\boldsymbol{\theta}) + \eta \|\hat{\delta}_{PK}^\theta\|_{L_2(\Omega)}^2.$$

We refer to the loss function (4.2) as the *penalized projected kernel loss function* (abbreviated as PPK loss function). By some direct calculations, we have that

$$(4.3) \quad \hat{\boldsymbol{\theta}}_{PPK} = \underset{\Theta}{\operatorname{argmin}} (\mathbf{Y} - \mathbf{Y}_{\theta^s})^T \Sigma^{-1} (\mathbf{Y} - \mathbf{Y}_{\theta^s}),$$

where $\Sigma^{-1} = \left[(\mathbf{K}_\theta + n\lambda \mathbf{I}_n)^{-1} + \gamma (\mathbf{K}_\theta + n\lambda \mathbf{I}_n)^{-1} \|K_\theta(\mathbf{x}, \mathbf{X})\|_{L_2(\Omega)}^2 (\mathbf{K}_\theta + n\lambda \mathbf{I}_n)^{-1} \right]$ and $\gamma = \eta/\lambda$. This expression provides a natural Bayesian interpretation of the penalized projected kernel calibration, i.e.

$$(4.4) \quad \pi(\boldsymbol{\theta} | \mathbf{Y}, \mathbf{Y}^s) \propto \pi(\boldsymbol{\theta}) \times \exp \left\{ -\frac{1}{2} (\mathbf{Y} - \mathbf{Y}_{\theta^s})^T (\mathbf{K}_\theta + n\lambda \mathbf{I}_n)^{-1} (\mathbf{Y} - \mathbf{Y}_{\theta^s}) \right\},$$

where

$$(4.5) \quad \pi(\boldsymbol{\theta}) \propto \exp \left\{ -\gamma/2 \int_{\Omega} \left(\hat{\delta}_{PK}^\theta(\mathbf{x}) \right)^2 d\mathbf{x} \right\}.$$

We can easily make a comparison between the projected kernel calibration and the proposed calibration from their Bayesian interpretations (2.8) and (4.4). Given the definition of $\boldsymbol{\theta}^*$, the estimation of $\boldsymbol{\theta}$ favors to values where $\|\hat{\delta}_{PK}^\theta\|_{L_2(\Omega)}^2$ is small. In turn, the prior distribution $\pi(\boldsymbol{\theta})$ of the proposed method is inversely proportional to $\|\hat{\delta}_{PK}^\theta\|_{L_2(\Omega)}^2$, which appears more suitable than the uninformative prior used in (2.8).

4.2. Asymptotic properties. In this section, we investigate the asymptotic properties of the proposed estimator. We first address the number of local minima of the PPK loss function, and then show that under certain conditions the proposed estimator of $\boldsymbol{\theta}$ is semi-parametrically efficient. Finally, we assess the predictive power of the proposed method in estimating the true process $\zeta(\cdot)$.

Theorem 4.1. *Under the conditions of Proposition 3.4, suppose there exist constants $U \geq L$, such that*

$$U \mathbf{E}_{\theta^s} \geq -\frac{\partial^2 L_2(\boldsymbol{\theta})}{\partial \boldsymbol{\theta} \partial \boldsymbol{\theta}^T} \Big|_{\boldsymbol{\theta}=\boldsymbol{\theta}^s} \geq L \mathbf{E}_{\theta^s}.$$

If $\eta \in \Gamma_\eta$, where $\Gamma_\eta \subset (0, \infty)$ is an interval determined by U and L . The specific form of Γ_η is given in (B.12), we have that asymptotically (i.e. for the sample size $n \rightarrow \infty$) $\boldsymbol{\theta}^s$ is a local minimum (maximum) of PPK loss function if $\boldsymbol{\theta}^s$ is a local minimum (maximum) of the L_2 loss function.

The theorem means that by choosing an appropriate value of η , we may avoid the problem of having too many local minima. Next, we turn to the asymptotic properties of $\hat{\boldsymbol{\theta}}_{PPK}$.

Theorem 4.2. *In addition to the assumptions of Proposition 3.4, assume that B1. The matrix*

$$\mathbf{V} = \int_{\Omega} \frac{\partial^2}{\partial \boldsymbol{\theta}^T \partial \boldsymbol{\theta}} (\zeta(\mathbf{x}) - y^s(\mathbf{x}, \boldsymbol{\theta}^*))^2 d\mathbf{x}$$

is positive definite.

B2. *There exists a neighborhood of $\boldsymbol{\theta}^*$, denoted as Θ' , satisfying*

$$\sup_{\boldsymbol{\theta} \in \Theta', j=1,2,\dots,q} \left\{ \left\| \frac{\partial y^s(\cdot, \boldsymbol{\theta})}{\partial \theta_j} \right\|_{\mathcal{N}_{K_\theta}(\Omega)} \right\} < \infty,$$

$$\sup_{\boldsymbol{\theta} \in \Theta', 1 \leq i, j \leq q} \left\{ \left\| \frac{\partial^2 y^s(\cdot, \boldsymbol{\theta})}{\partial \theta_i \partial \theta_j} \right\|_{\mathcal{N}_{K_\theta}(\Omega)} \right\} < \infty.$$

Then we have

$$(4.6) \quad \hat{\boldsymbol{\theta}}_{PPK} - \boldsymbol{\theta}^* = 2\mathbf{V}^{-1} \left\{ \frac{1}{n} \sum_{i=1}^n \epsilon_i \frac{\partial y^s(\mathbf{x}_i, \boldsymbol{\theta}^*)}{\partial \boldsymbol{\theta}} \right\} + o_p(n^{-1/2}).$$

Theorem 4.2 shows the asymptotic normality of $\hat{\boldsymbol{\theta}}_{PPK}$:

$$\sqrt{n}(\hat{\boldsymbol{\theta}}_{PPK} - \boldsymbol{\theta}^*) \sim N(\mathbf{0}, 4\sigma^2 \mathbf{V}^{-1} \mathbf{E}_{\boldsymbol{\theta}^*} \mathbf{V}^{-1}).$$

It is worth noticing that, the asymptotic representation of $\hat{\boldsymbol{\theta}}_{PPK} - \boldsymbol{\theta}^*$ agrees with Theorem 4.3 of [24]. It also shows that the penalized projected kernel calibration is semi-parametrically efficient.

Let $\hat{\zeta}_n(\cdot) = \hat{\delta}_{PPK}^{\hat{\boldsymbol{\theta}}_{PPK}}(\cdot) + y^s(\cdot, \hat{\boldsymbol{\theta}}_{PPK})$, then $\hat{\zeta}_n$ is a natural estimator of ζ . Theorem 4.3 gives the predictive power of the proposed method.

Theorem 4.3. *Under the conditions of Theorem 4.2, we have*

$$(4.7) \quad \|\hat{\zeta}_n - \zeta\|_{L_2(\Omega)} = O_p(n^{-\frac{m}{2m+d}}).$$

The rate of convergence in (4.7) equals the minimax rate in the current context [22].

5. Addressing computational problems. Evaluating $\hat{\boldsymbol{\theta}}_{PPK}$ has two major difficulties in practice. The first problem is the calculations of projected kernels, since it is hard to evaluate K_θ from its definition (2.2). The second problem is the choice of η . We focus on these problems in this section.

5.1. Calculus for projected kernels. Let $\mathbf{g}_\theta^T(\cdot) = \frac{\partial y^s(\cdot, \boldsymbol{\theta})}{\partial \boldsymbol{\theta}}$ and $\mathbf{h}_\theta(\mathbf{x}) = \langle K(\mathbf{x}, \cdot), \mathbf{g}_\theta(\cdot) \rangle_{L_2(\Omega)}$. A closed form for K_θ is derived in this subsection. Because \mathbf{E}_θ is positive definite, it follows from basic linear algebra that

$$(5.1) \quad \begin{aligned} \mathcal{P}_{\mathcal{G}_\theta}^{(1)} K(\mathbf{x}_1, \mathbf{x}_2) &= \mathcal{P}_{\mathcal{G}_\theta}^{(2)} K(\mathbf{x}_2, \mathbf{x}_1) = \mathbf{h}_\theta^T(\mathbf{x}_2) \mathbf{E}_\theta^{-1} \mathbf{g}_\theta(\mathbf{x}_1), \\ \mathcal{P}_{\mathcal{G}_\theta}^{(1)} \mathcal{P}_{\mathcal{G}_\theta}^{(2)} K(\mathbf{x}_1, \mathbf{x}_2) &= \mathbf{g}_\theta^T(\mathbf{x}_2) \mathbf{E}_\theta^{-1} \mathbf{H}_\theta \mathbf{E}_\theta^{-1} \mathbf{g}_\theta(\mathbf{x}_1), \end{aligned}$$

where $\mathbf{H}_\theta = \int \int K(\mathbf{t}_1, \mathbf{t}_2) \mathbf{g}_\theta(\mathbf{t}_1) \mathbf{g}_\theta^T(\mathbf{t}_2) d\mathbf{t}_1 d\mathbf{t}_2$. Let $\mathbf{w}_\theta(\mathbf{x}) = \mathbf{H}_\theta \mathbf{E}_\theta^{-1} \mathbf{g}_\theta(\mathbf{x}) - \mathbf{h}_\theta(\mathbf{x})$, then $K_\theta(\mathbf{x}_1, \mathbf{x}_2)$ (2.2) can be represented as

$$(5.2) \quad K(\mathbf{x}_1, \mathbf{x}_2) + \mathbf{w}_\theta(\mathbf{x}_1)^T \mathbf{H}_\theta^{-1} \mathbf{w}_\theta(\mathbf{x}_2) - \mathbf{h}_\theta^T(\mathbf{x}_1) \mathbf{H}_\theta^{-1} \mathbf{h}_\theta(\mathbf{x}_2).$$

Tuo [24] points out that, projected kernel calibration is similar to the Bayesian calibration method proposed by [15], which is based on an orthogonal Gaussian process (OGP) modeling technique. The covariance function of an orthogonal Gaussian process which is defined as (5.3) is a projected kernel function.

$$(5.3) \quad K_{or}(\mathbf{x}_1, \mathbf{x}_2) = K(\mathbf{x}_1, \mathbf{x}_2) - \mathbf{h}_\theta^T(\mathbf{x}_1) \mathbf{H}_\theta^{-1} \mathbf{h}_\theta(\mathbf{x}_2).$$

By comparing (5.2) with (5.3), we have that, if and only if $\mathbf{w}_\theta(\mathbf{x}) = \mathbf{0}$, there is $K_\theta = K_{or}$. To address the difficult integrations, we refer to [15] and approximate $\langle f_1, f_2 \rangle_{L_2(\Omega)}$ by

$$(5.4) \quad \frac{1}{N} \sum_{k=1}^N f_1(\xi_k) f_2(\xi_k),$$

where ξ_k 's are independent random samples from the uniform distribution over Ω . By the strong law of large numbers, (5.4) almost surely converges to $\langle f_1, f_2 \rangle_{L_2(\Omega)}$ as $N \rightarrow \infty$. Through this approximation, $\mathbf{h}_\theta(\mathbf{x})$, \mathbf{E}_θ^{-1} and \mathbf{H}_θ can be represented as

$$(5.5) \quad \begin{aligned} \mathbf{h}_\theta(\mathbf{x}) &= \frac{1}{N} \sum_{k=1}^N K(\mathbf{x}, \xi_k) \mathbf{g}_\theta(\xi_k), \\ \mathbf{E}_\theta &= \frac{1}{N} \sum_{k=1}^N \mathbf{g}_\theta(\xi_k) \mathbf{g}_\theta^T(\xi_k), \\ \mathbf{H}_\theta &= \frac{1}{N^2} \sum_{i=1}^N \sum_{j=1}^N K(\xi_i, \xi_j) \mathbf{g}_\theta(\xi_i) \mathbf{g}_\theta^T(\xi_j). \end{aligned}$$

5.2. Choice of η . The choice of the tuning parameter η affects the number of local optima of $L_{PPK}(\boldsymbol{\theta})$. In particular, by increasing η from 0 to ∞ , one may gradually turn $L_{PPK}(\boldsymbol{\theta})$ from rough to smooth. In this subsection, a BIC-like criterion is introduced to choose η .

Let $\text{RI}(L)$ be an indicator that measure the ruggedness of a loss function L , such as the number of local optimal points. This indicator satisfies that:

- $\text{RI}(L) \geq 0$, and the equality holds if and only if the loss function L is a nonnegative constant;
- $\text{RI}(C_2 L) = \text{RI}(L)$, where $C_2 > 0$ is a constant;
- $\text{RI}(L + C_3) = \text{RI}(L)$, where $C_3 > 0$ is a constant;
- If $\text{RI}(L_1) \leq \text{RI}(L_2)$ then $\text{RI}(L_1) \leq \text{RI}(L_1 + L_2) \leq \text{RI}(L_2)$.

Theorem 3.9 says that when the L_2 loss function has more than one local extrema, $L_{PK}(\boldsymbol{\theta})$ tends to have more local extrema than $\|\hat{\delta}_{PK}^\theta\|_{L_2(\Omega)}^2$. Therefore, it is easy to see that, $\text{RI}(L_{PK}(\boldsymbol{\theta})) \geq \text{RI}(L_{PPK}(\boldsymbol{\theta})) \geq \text{RI}(\|\hat{\delta}_{PK}^\theta\|_{L_2(\Omega)}^2)$, with $\text{RI}(L_{PPK})$ being a decreasing function of η .

We may thus use a BIC-like criterion to estimate η as follows

$$(5.6) \quad \eta = \underset{\eta}{\operatorname{argmin}} \log(L_{PK}(\hat{\boldsymbol{\theta}}_{PPK})) + \operatorname{RI}(L_{PPK}) \log(n)/n.$$

In the field of optimization, there are many indicators that may be used to measure the smoothness of the objective function [23]. A natural choice among these indicators is the number of local optima of the objective function. Upon denoting the number of local optima of the loss function L by $NLO(L)$, we have that

$$(5.7) \quad NLO(L) = \#\{\boldsymbol{\theta} : \frac{\partial L(\boldsymbol{\theta})}{\partial \boldsymbol{\theta}^T} = \mathbf{0}\}.$$

In most cases, one cannot find a closed form for $\frac{\partial L(\boldsymbol{\theta})}{\partial \boldsymbol{\theta}^T}$. By numerically approximating [21] the first derivative of L on $\boldsymbol{\theta}$, one may use Newton-Raphson method [19] to evaluate the number of local optima of the loss function L . If the tuning parameter η is chosen according to the NLO index, L_{PPK} is termed as PPK.NLO loss function.

Notice that when the dimension of $\boldsymbol{\theta}$ is large, it is always hard to count the number of local extrema of a loss function. In turn, amplitude indices which measure the distribution of local minima of the loss function L , are widely used to assess the smoothness of a function [23]. We employ the following definition

$$(5.8) \quad \operatorname{Amp}(L) = \frac{\max_{\boldsymbol{\theta}} L(\boldsymbol{\theta}) - \min_{\boldsymbol{\theta}} L(\boldsymbol{\theta})}{\int_{\Theta} L(\boldsymbol{\theta}) - \min_{\boldsymbol{\theta}} L(\boldsymbol{\theta}) d\boldsymbol{\theta}}.$$

The larger is $\operatorname{Amp}(L)$, the harder is to find the optimal point for the loss function L . The PPK loss function where η is chosen by the Amp index is referred to as PPK.Amp loss function. Let us denote by $\Theta_s = \{\boldsymbol{\theta}_1, \dots, \boldsymbol{\theta}_{N'}\}$ a discrete set of values of $\boldsymbol{\theta}$, where $\boldsymbol{\theta}_k, k = 1, \dots, N'$ is randomly sampled from the uniform distribution over Θ . We approximate $\operatorname{Amp}(L)$ by

$$(5.9) \quad \frac{\max_{\Theta_s} L(\boldsymbol{\theta}) - \min_{\Theta_s} L(\boldsymbol{\theta})}{\frac{1}{N'} \sum_{i=1}^{N'} [L(\boldsymbol{\theta}_i) - \min_{\Theta_s} L(\boldsymbol{\theta})]}.$$

6. Numerical studies. In this section, we examine the performance of the penalized projected kernel calibration by using two simulated examples and one real case study. In subsection 6.1, we go back to the example already discussed in 3.3, whereas in subsection 6.2, we study a simulated example with a two-dimensional calibration parameter. We compare the performance of the penalized projected kernel calibration with some commonly used calibration methods using samples with sizes. To ensure a fair comparison, the mean function, correlation function, as well as the $\{\xi_j\}$'s in the integration are the same.

6.1. Review of example 3.3. To assess the performance of the proposed method, we compare the PPK loss function with the L_2 loss function and the PK loss function when the sample sizes are $n = \{6, 15, 100\}$. The physical design and kernel function are the same as in 3.3. The tuning parameter η in the PPK loss function is chosen by the BIC-like criterion (5.6). We use the two quantities $NLO(L)$ and $\operatorname{Amp}(L)$ to quantify the smoothness of the loss function.

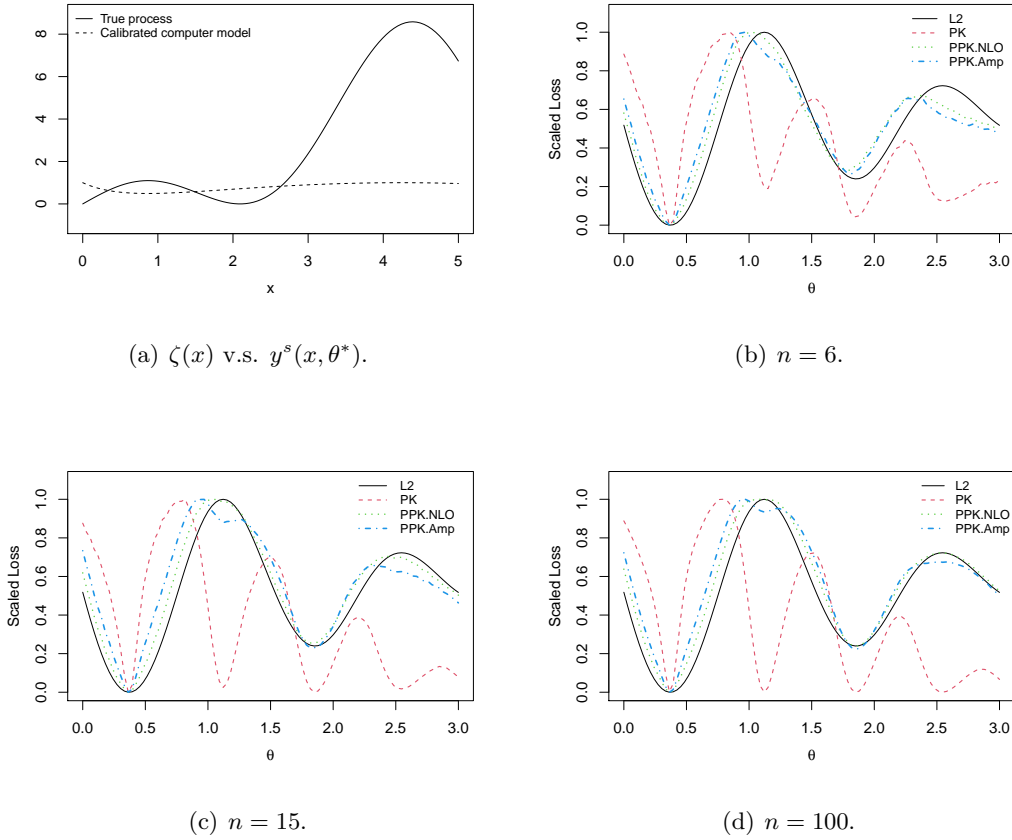


Figure 3. (a) the true process $\zeta(x)$ (black real line) v.s. the calibrated computer model $y^s(x, \theta^*)$ (black dashed line); (b)-(d) L_2 loss function (black real line) v.s. PK loss function (red dashed line) v.s. PPK. NLO loss function (green dotted line) v.s. PPK. Amp loss function (blue dot-dash line).

Looking at Fig. 3-(a), one may see that even though θ^* is the global minima of $\|\zeta - y^s(\cdot, \theta)\|_{L_2(\Omega)}^2$, the discrepancy between the true process and the calibrated computer model is still large. Figs. 3-(b-d) provide a comparison among the different loss functions when the sample sizes are 6, 15 and 100. PPK. NLO loss function is the PPK loss function determined by using the NLO index, whereas PPK.Amp loss is that found using the Amp index. Since we have a single parameter, we use the package *rootSolve* [19] in R to obtain the number of local optima of the loss function and the estimation of η_{NLO} . Let $\Theta_s = \{\theta_1, \dots, \theta_{N'}\}$ where $\theta_i = \frac{3i}{N'}$ and $N' = 100$. By approximating $Amp(L)$ using (5.9), we obtain η_{Amp} . Table 2 summarizes results for η_{NLO} and η_{Amp} at different sample sizes.

Figure 3 shows that when the sample size is larger than 6, the PPK loss function has several extrema. Figure 3-(b) shows that when the sample size is 6, one may discriminate the global minimum from the local minimum near 1.855 by an effective optimization algorithm. However, Figs. 3-(c-d) show that when the sample size is larger than 15, it becomes extremely

Table 2
Choice of η

Sample size	η_{NLO}	η_{Amp}
$n = 6$	0.153	0.0503
$n = 15$	0.705	0.236
$n = 100$	13.632	6.477

hard to find the global minimum by any optimization algorithm. It can be seen that using the PPK loss function solves this problem. The number of local optima for the PPK.NLO loss functions is 4, and the values of the local minima are different. Although the PPK.Amp loss functions have more than 4 local optimal points, the global minimizer may be evaluated effectively by some optimization method, e.g. the quasi-Newton optimization methods with multiple initial points.

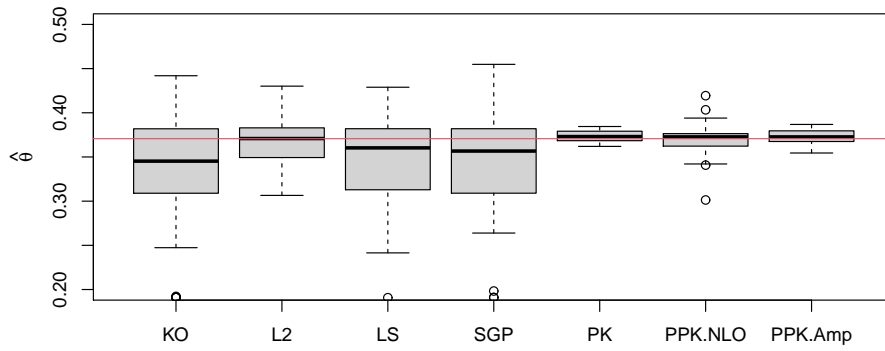
As it follows from its definition, and from the fact that $NLO(L)$ counts the number of local optima, the BIC-like criterion looks for values of η that decrease the number of local optimal points of the PPK loss function. As a consequence, η_{NLO} is larger than η_{Amp} as shown in Table 2, and PPK.NLO loss functions have less local optima than the PPK.Amp one, as shown in Figure 3. Moreover, η_{NLO} and η_{Amp} are increasing with the sample size. The reason is that it becomes much harder to pick out the global minimum of the PK loss function for increasing n .

Let us now compare the performance of the PPK calibration with that of KO's calibration (KO), L_2 calibration (L_2), least square calibration (LS), scaled Gaussian process model calibration (SGP), and projected kernel calibration (PK). To this aim, we repeat the process of calibration 100 times for each method, and show the box-plots of $\hat{\theta}$ in Figure 4. Since the PK calibration is easily trapped in a local optimal solution of the PPK loss function, we narrow the search space of the PK calibration to $[0, 0.5]$.

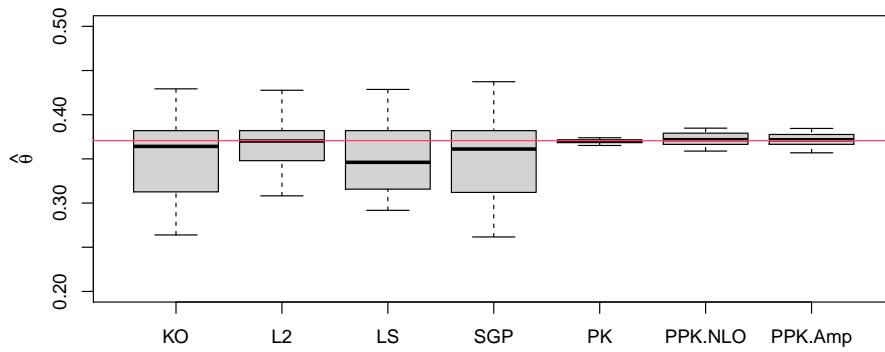
From Fig. 4, we can see that the variance of $\hat{\theta}_{PK}$ is the smallest. In fact, as the PK loss function tends to have more local optima, the PK loss function near its global minimum point is "sharp" (the derivative near the global minimum point is large). We also see that the bias of $\hat{\theta}_{PK}$ is close to zero. These results indicate that if the search region is narrowed, the PK calibration is clearly superior to the other methods. However, when there are many local optima in the search region, the PK calibration loses its advantages.

When the sample size is 6 and 15, the slower convergence speed leads to poor performance of the $\hat{\theta}_{SGP}$. When the sample size is 100, we can still see substantial estimation errors in $\hat{\theta}_{KO}$, the reason is that the discrepancy δ is large (see Figure 3-(a)) and $\hat{\theta}_{KO}$ is inconsistent.

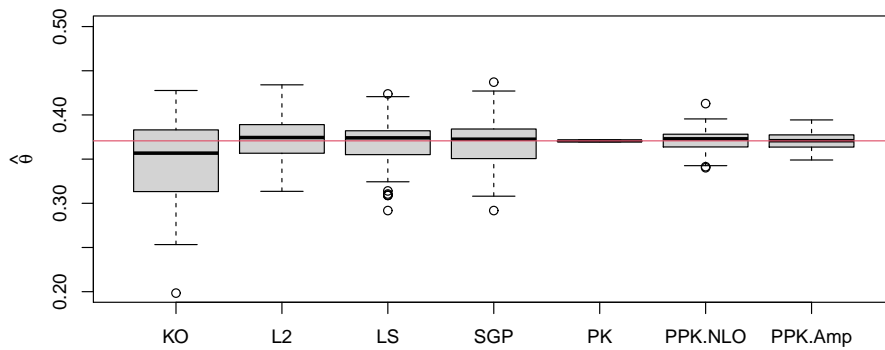
If we denote the estimate obtained from PPK.NLO (PPK.Amp) as $\hat{\theta}_{PPK.NLO}$ ($\hat{\theta}_{PPK.Amp}$), we have that the bias of $\hat{\theta}_{PPK}$ is close to zero. The variance of $\hat{\theta}_{PPK}$ is smaller than the variance of $\hat{\theta}$ given by other methods, except that from the PK calibration method. In addition, because the tuning parameter $\eta_{Amp} < \eta_{NLO}$, the $\hat{\theta}_{PPK.Amp}$'s are closer to $\hat{\theta}_{PK}$, and the variance of $\hat{\theta}_{PPK.Amp}$ is smaller than the variance of $\hat{\theta}_{PPK.NLO}$. It implies that our proposed method outperforms the other calibration methods.



(a) $n = 6$.



(b) $n = 15$.



(c) $n = 100$.

Figure 4. Estimations of the calibration parameter by different methods.

6.2. Low-accuracy version of the PARK function [34]. Assume that $\zeta(\cdot)$ is the PARK function [14],

$$\zeta(\mathbf{x}) = \frac{x_1}{2} \left[\sqrt{1 + (x_2 + x_3^2) \frac{x_4}{x_1^2}} - 1 \right] + (x_1 + 3x_4) \exp[1 + \sin(x_3)], \mathbf{x} \in [0, 1]^4.$$

In Ref. [34] a lower accuracy version of the PARK function is used for the purpose of multi-fidelity simulation. Assuming that some constants of this lower fidelity model are to be determined, we use following computer model to examine the performance of the proposed method:

$$y^s(\mathbf{x}, \boldsymbol{\theta}) = (\theta_1 + \frac{\sin(x_1)}{10})\zeta(\mathbf{x}) + \theta_2(-2x_1 + x_2^2 + x_3^2) + 0.5,$$

where θ_1 and θ_2 are two calibration parameters, with $\boldsymbol{\theta} \in [-5, 5]^2$.

Let $\mathbf{X} = (\mathbf{x}_1, \dots, \mathbf{x}_n)^T$ be the physical design, which is randomly generated by maximin Latin hypercube design method [17]. Suppose the observation error ϵ_i 's are mutually independent and distributed as $N(0, 0.1^2)$. We use a Matérn kernel function (2.1) with $\nu = 7/2$ as the kernel function K . To determine the hyper-parameter ρ in (2.1), for fixed $\boldsymbol{\theta}_0$, we build a Gaussian-process model to approximate $y(\mathbf{x}_i) - y^s(\mathbf{x}_i, \boldsymbol{\theta}_0)$ and estimate ρ by using maximum likelihood. Because the least square estimator $\hat{\boldsymbol{\theta}}_{LS}$ proposed in [32] is consistent, we set $\boldsymbol{\theta}_0 = \hat{\boldsymbol{\theta}}_{LS}$.

Contour maps of the L_2 and the PK loss functions with $n = \{10, 20, 100\}$ are shown in Figure 5. From the top left subfigure, we can see that, $\boldsymbol{\theta}^*$ is the only local optimal point of the L_2 loss function. The top right subfigure, and the two lower subfigures, show that the PK loss function has only one local minimum, regardless of the sample size. This indicates that when the L_2 loss function has only one local optimal point, the PK loss function is not affected by the multiple local minima problem. Since the L_2 and the PPK loss functions are convex, we apply the NEWUOA algorithm [16] to find $\boldsymbol{\theta}^*$ and $\hat{\boldsymbol{\theta}}_{PK}$. In Fig. 5, $\boldsymbol{\theta}^* = (0.546, 0.0926)$ and the $\hat{\boldsymbol{\theta}}_{PK}$ are denoted by a blue cross and by red triangles, respectively. By comparing the locations of the red triangles with that of the blue cross, we have that, $\hat{\boldsymbol{\theta}}_{PK}$ is very close to $\boldsymbol{\theta}^*$ especially then n is large.

To compare the performance of the proposed method with some existing calibration methods, we repeat the simulation procedure 100 times to assess the average performance of different methods.

Figure 6 illustrates the estimation results of the different calibration methods. Since there is only one local optimal point in the PK loss function, the choice of η is zero, therefore $\hat{\boldsymbol{\theta}}_{PPK} = \hat{\boldsymbol{\theta}}_{PK}$. We can see that when the sample size is 10 and 20, the bias of $\hat{\boldsymbol{\theta}}_{PK}$ is the smallest, whereas the variance of $\hat{\boldsymbol{\theta}}_{PK}$ is slightly larger than $\hat{\boldsymbol{\theta}}_{LS}$. When the sample size is 100, all the methods perform well except the KO's calibration.

6.3. Spot welding example. Let us now consider the spot welding example studied in [1] and [33]. Analogously to [33], we consider two control variables: the load and the current. Besides the control variables in the physical experiment, the computer model (a Finite Element model) also involves a calibration parameter (denoted as u in [1]). Details of the inputs and outputs of the computer experiments are listed in Table 3. The physical data are listed in Table 4 of [1]. There are 21 available runs for the computer code, as presented in Table 3 of

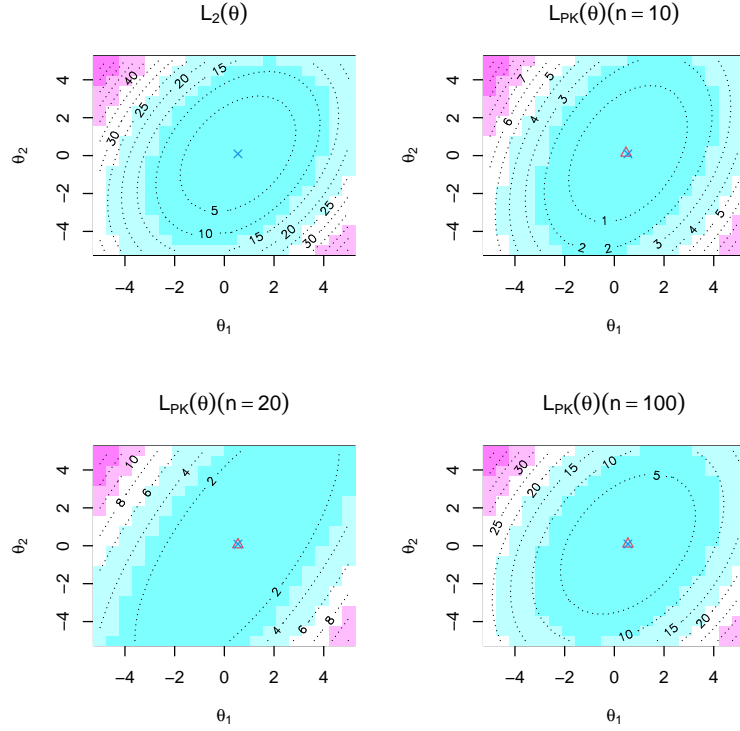


Figure 5. L_2 loss function v.s. PK loss function with $n = \{10, 20, 100\}$ in Example 6.2. The cross in each subfigure is the location of θ^* , and triangle is the location of θ_{PK} .

Table 3

Inputs and output of the computer experiments

Inputs		
C (current)	[23, 30]	control variable
L (load)	[3.8, 5.5]	control variable
θ (contact resistance)	[0.8, 8]	calibration parameter
Output		
	Size of the nugget after 8-cycles	

[1]. With the help of the RobustGaSP package [3] in R, a Gaussian process model is built to approximate the computer outputs. In the process of calibration, the Finite Element model is replaced by the predictive mean of the RobustGaSP emulator. Since there is only one local optimal point in the PK loss function, also here we have $\eta = 0$.

The computer models calibrated by the proposed method, together with their corresponding point-wise 95%-credible intervals, are depicted in Figure 7. We can see that the proposed method provides a well calibrated computer model.

7. Discussion. In this work, we have proven that the projected kernel calibration may be easily trapped in local minima of the L_2 loss between the true process and the computer model (or even in local maxima). A frequentist calibration method has been proposed to overcome

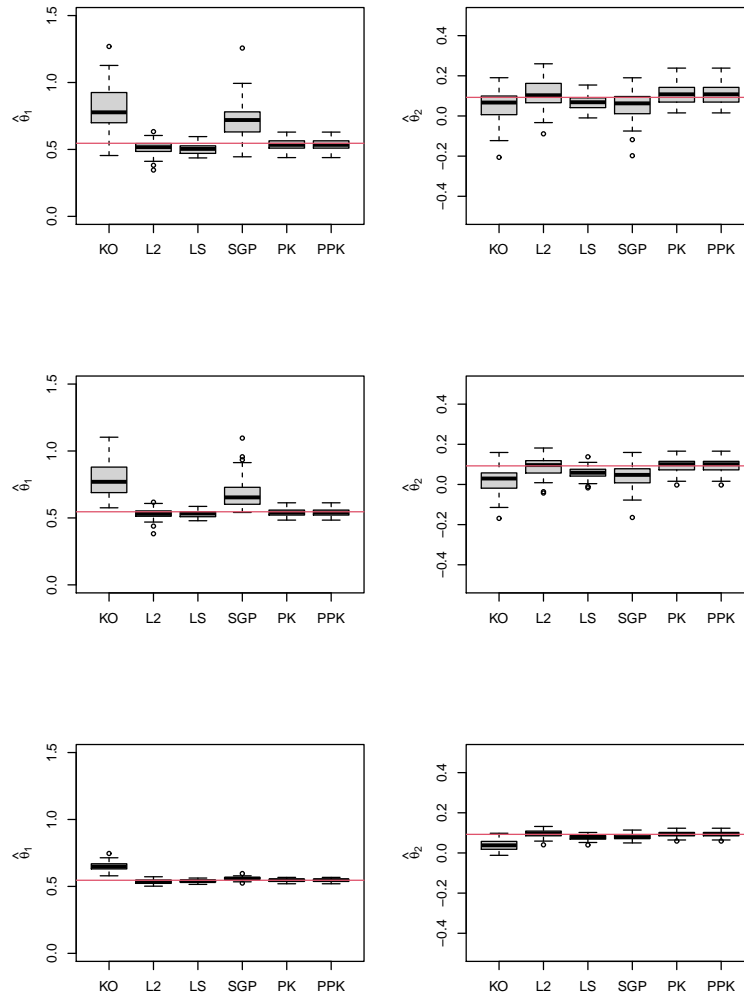


Figure 6. Comparisons of different calibration methods with the sample size $n = 10$ (the first row), $n = 20$ (the second row) and $n = 100$ (the third row).

this problem. The estimators of the calibration parameters given by the proposed method are consistent and semi-parametrically efficient. Numerical examples have been studied to compare the proposed methods with some existing calibration methods, and results show that our method outperforms the others.

The proposed method suggests a Monte Carlo method (5.4) to approximate the L_2 inner products. However, there is no guarantee that the numerical estimator based on the Monte Carlo approximation is close enough to the theoretical estimator (4.3). This will require further work.

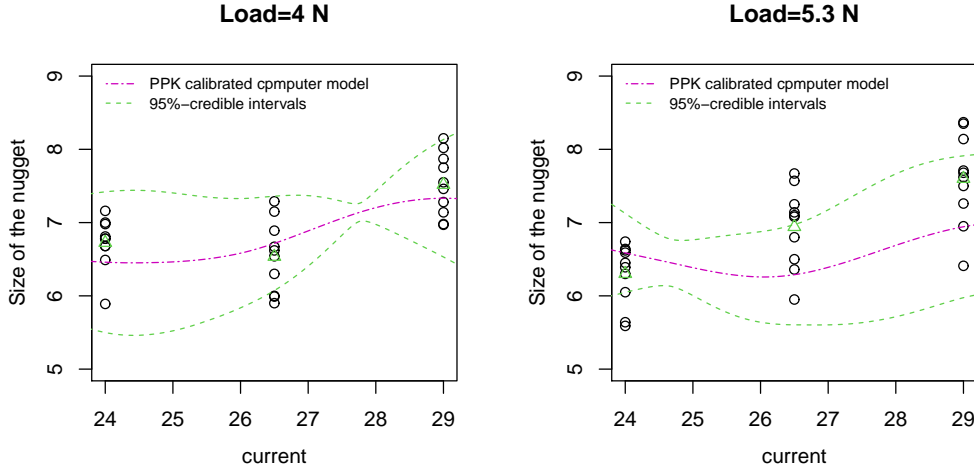


Figure 7. Physical observations (black circles); mean of physical observations for a fixed current (green triangles); mean of the calibrated computer model by the proposed method (red real line) and the 95% interval of the calibrated computer model (green dashed line).

In this work, we assume that all possible functions of interest belong to the reproducing kernel Hilbert space $\mathcal{N}_K(\Omega)$ generated by the kernel function K . We also assume that the space $\mathcal{N}_K(\Omega)$ can be embedded into the Sobolev space $H^m(\Omega)$ with $m > d/2$. In other words, we are mainly concerned with the reproducing kernel Hilbert spaces generated by the smooth kernel functions. Rough kernel functions such as those generated by the rough fractional maximal and integral operators [6, 9] and the Schrödinger operators [7, 8, 10], etc. are not covered in this paper. The results for calibration with the rough kernel functions need further investigation.

Appendix A. Technical proofs in Section 3. In this section, we prove the propositions and theorems in Section 3.

A.1. Proof of Proposition 3.1.

Proof. Following from the generalized representer's theorem [18], $\hat{\delta}_{PK}^\theta$ can be represented by

$$(A.1) \quad \hat{\delta}_{PK}^\theta(\mathbf{x}) = K_\theta^T(\mathbf{x}, \mathbf{X})(\mathbf{K}_\theta + n\lambda\mathbf{I}_n)^{-1}(\mathbf{Y} - \mathbf{Y}_\theta^s).$$

Therefore the norm of $\hat{\delta}_{PK}^\theta$ in $\mathcal{N}_{K_\theta}(\Omega)$ is given by

$$(A.2) \quad \|\hat{\delta}_{PK}^\theta\|_{\mathcal{N}_{K_\theta}(\Omega)}^2 = (\mathbf{Y} - \mathbf{Y}_\theta^s)^T (\mathbf{K}_\theta + n\lambda\mathbf{I}_n)^{-1} \mathbf{K}_\theta (\mathbf{K}_\theta + n\lambda\mathbf{I}_n)^{-1} (\mathbf{Y} - \mathbf{Y}_\theta^s).$$

Moreover, because the vector $(\hat{\delta}_{PK}^\theta(\mathbf{x}_1), \dots, \hat{\delta}_{PK}^\theta(\mathbf{x}_n))^T$ can be expressed by

$$\mathbf{K}_\theta (\mathbf{K}_\theta + n\lambda\mathbf{I}_n)^{-1} (\mathbf{Y} - \mathbf{Y}_\theta^s).$$

It yields

$$(A.3) \quad \frac{1}{n} \sum_{i=1}^n (\delta_i^\theta - \hat{\delta}_{PK}^\theta(\mathbf{x}_i))^2 = n\lambda^2 (\mathbf{Y} - \mathbf{Y}_\theta^s)^T (\mathbf{K}_\theta + n\lambda \mathbf{I}_n)^{-2} (\mathbf{Y} - \mathbf{Y}_\theta^s).$$

Combining (A.2) with (A.3), we obtain that

$$\frac{1}{n} \sum_{i=1}^n (\delta_i^\theta - \hat{\delta}_{PK}^\theta(\mathbf{x}_i))^2 + \lambda \|\hat{\delta}_{PK}^\theta\|_{\mathcal{N}_{K_\theta}(\Omega)}^2 = \lambda (\mathbf{Y} - \mathbf{Y}_\theta^s)^T (\mathbf{K}_\theta + n\lambda \mathbf{I}_n)^{-1} (\mathbf{Y} - \mathbf{Y}_\theta^s),$$

which implies the desired result. ■

A.2. Proof of Proposition 3.2.

Proof. Because $\mathcal{G}_\theta \subset \mathcal{N}_K(\Omega)$ is finite dimensional, based on the generalized representer's theorem [18], $\hat{\delta}^\theta$ can be represented as

$$(A.4) \quad \hat{\delta}^\theta(\mathbf{x}) = \sum_{i=1}^n \alpha_i^\theta K_\theta(\mathbf{x}, \mathbf{x}_i) + \sum_{j=1}^q \beta_j^\theta \frac{\partial y^s(\mathbf{x}, \boldsymbol{\theta})}{\partial \theta_j},$$

with $\boldsymbol{\alpha}^\theta = (\alpha_1^\theta, \dots, \alpha_n^\theta)^T$ and $\boldsymbol{\beta}^\theta = (\beta_1^\theta, \dots, \beta_q^\theta)^T$ defined as

$$\boldsymbol{\alpha}^\theta = (\mathbf{K}_\theta + n\lambda \mathbf{I}_n)^{-1} (\mathbf{Y} - \mathbf{Y}_\theta^s),$$

and

$$\boldsymbol{\beta}^\theta = (\mathbf{G}_\theta \mathbf{G}_\theta^T)^{-1} \mathbf{G}_\theta (\mathbf{Y} - \mathbf{Y}_\theta^s),$$

respectively. Here \mathbf{G}_θ is a $q \times n$ matrix, with $[\mathbf{G}_\theta]_{j,i} = \frac{\partial y^s(\mathbf{x}_i, \boldsymbol{\theta})}{\partial \theta_j}$, $j = 1, \dots, q; i = 1, \dots, n$ and $q \leq n$.

From (A.4), we can easily have that

$$\mathcal{P}_{\mathcal{G}_\theta}^\perp \hat{\delta}^\theta = \sum_{i=1}^n \alpha_i^\theta K_\theta(\mathbf{x}, \mathbf{x}_i),$$

which implies the desired results. ■

A.3. Proof of Proposition 3.4.

Proof. Because $\hat{\delta}^\theta$ is a minimizer of

$$(A.5) \quad l_\theta(g_0) = \frac{1}{n} \sum_{i=1}^n (\delta_i^\theta - \mathcal{P}_{\mathcal{G}_\theta} g_0(\mathbf{x}_i))^2 + \frac{1}{n} \sum_{i=1}^n (\delta_i^\theta - \mathcal{P}_{\mathcal{G}_\theta}^\perp g_0(\mathbf{x}_i))^2 + \lambda \|\mathcal{P}_{\mathcal{G}_\theta}^\perp g_0\|_{\mathcal{N}_{K_\theta}(\Omega)}^2,$$

where $g_0 \in \mathcal{N}_K(\Omega)$, we have the following basic inequality

$$\begin{aligned} & \frac{1}{n} \sum_{i=1}^n (\delta_i^\theta - \mathcal{P}_{\mathcal{G}_\theta} \hat{\delta}^\theta(\mathbf{x}_i))^2 + \frac{1}{n} \sum_{i=1}^n (\delta_i^\theta - \hat{\delta}_{PK}^\theta(\mathbf{x}_i))^2 + \lambda \|\hat{\delta}_{PK}^\theta\|_{\mathcal{N}_{K_\theta}(\Omega)}^2 \\ & \leq \frac{1}{n} \sum_{i=1}^n (\delta_i^\theta - \mathcal{P}_{\mathcal{G}_\theta} \delta^\theta(\mathbf{x}_i))^2 + \frac{1}{n} \sum_{i=1}^n (\delta_i^\theta - \mathcal{P}_{\mathcal{G}_\theta}^\perp \delta^\theta(\mathbf{x}_i))^2 + \lambda \|\mathcal{P}_{\mathcal{G}_\theta}^\perp \delta^\theta\|_{\mathcal{N}_{K_\theta}(\Omega)}^2. \end{aligned}$$

With some simple calculations, the basic inequality can be expressed as

$$(A.6) \quad 2 \left\langle \mathcal{P}_{\mathcal{G}_\theta}^\perp \delta^\theta - \hat{\delta}_{PK}^\theta, \mathcal{P}_{\mathcal{G}_\theta} \delta^\theta \right\rangle_n + 2 \left\langle \mathcal{P}_{\mathcal{G}_\theta} (\delta^\theta - \hat{\delta}^\theta), \mathcal{P}_{\mathcal{G}_\theta}^\perp \hat{\delta}^\theta \right\rangle_n + \left\| \delta^\theta - \hat{\delta}^\theta \right\|_n^2 + \lambda \left\| \hat{\delta}_{PK}^\theta \right\|_{\mathcal{N}_{K_\theta}(\Omega)}^2 \\ \leq \lambda \left\| \mathcal{P}_{\mathcal{G}_\theta}^\perp \delta^\theta \right\|_{\mathcal{N}_{K_\theta}(\Omega)}^2 + 2 \left| \left\langle \delta^\theta - \hat{\delta}^\theta, \epsilon \right\rangle_n \right|.$$

For the first and the second terms on the left side of the basic inequality, because x_i 's follow the uniform distribution over Ω , there is an asymptotic equivalence relation between the L_2 and the empirical norm [24]:

$$(A.7) \quad \lim_{n \rightarrow \infty} \sup P \left\{ \sup_{\|g\|_{\mathcal{N}_K(\Omega)} = O_p(1), \|g\|_{L_2(\Omega)} > \tau n^{-\frac{m}{2m+d}}/\eta} \left| \frac{\|g\|_n}{\|g\|_{L_2(\Omega)}} - 1 \right| \geq \eta \right\} = 0.$$

As a result, we have that

$$(A.8) \quad \left\langle \mathcal{P}_{\mathcal{G}_\theta}^\perp \delta^\theta - \hat{\delta}_{PK}^\theta, \mathcal{P}_{\mathcal{G}_\theta} \delta^\theta \right\rangle_n + \left\langle \mathcal{P}_{\mathcal{G}_\theta} (\delta^\theta - \hat{\delta}^\theta), \mathcal{P}_{\mathcal{G}_\theta}^\perp \hat{\delta}^\theta \right\rangle_n = o_p(n^{-1/2}).$$

For the first term on the right side of the basic inequality, following from the Theorem 3.3 in [24] and together with the condition (A3), we have that, there is a constant $a_1 > 0$ such that

$$(A.9) \quad \left\| \mathcal{P}_{\mathcal{G}_\theta}^\perp \delta^\theta \right\|_{\mathcal{N}_{K_\theta}(\Omega)}^2 \leq b_1^2 \left\| \delta^\theta \right\|_{\mathcal{N}_K(\Omega)}^2 \leq a_1.$$

where

$$b_1 = 1 + \sup_{g \in \mathcal{G}_\theta, \|g\|_{L_2(\Omega)} = 1} \|g\|_{\mathcal{N}_K(\Omega)} \|g\|_{L_2(\Omega)} < K, g \in \mathcal{G}_\theta, \|g\|_{L_2(\Omega)} = 1.$$

For the second term on the right side of the basic inequality, following from the Theorem 5.11 in [28], we obtain the modulus of continuity of the empirical process $v(g') = \langle \epsilon, g' - g \rangle_n$ as

$$\sup_{g \in \mathcal{N}_K(\Omega)} \frac{|\langle \epsilon, g' - g \rangle_n|}{\|g - g'\|_n^{1-\frac{d}{2m}} \|g'\|_{\mathcal{N}_K(\Omega)}^{d/2m}} = O_p(n^{-1/2}).$$

That is, there is a constant $a_2 > 0$ such that

$$(A.10) \quad \left| \langle \delta^\theta - \hat{\delta}^\theta, \epsilon \rangle_n \right| \\ \leq \frac{a_2}{2} n^{-1/2} \left\| \delta^\theta - \hat{\delta}^\theta \right\|_n^{1-\frac{d}{2m}} \left\| \hat{\delta}^\theta \right\|_{\mathcal{N}_K(\Omega)}^{d/2m},$$

By combining (A.6)-(A.10), we have that

$$(A.11) \quad \left\| \delta^\theta - \hat{\delta}^\theta \right\|_n^2 + \lambda \left\| \hat{\delta}_{PK}^\theta \right\|_{\mathcal{N}_{K_\theta}(\Omega)}^2 \leq a_1 \lambda + a_2 n^{-1/2} \left\| \delta^\theta - \hat{\delta}^\theta \right\|_n^{1-\frac{d}{2m}} \left\| \hat{\delta}^\theta \right\|_{\mathcal{N}_K(\Omega)}^{d/2m}.$$

Clearly, (A.11) implies either

$$\left\| \delta^\theta - \hat{\delta}^\theta \right\|_n^2 + \lambda \|\hat{\delta}_{PK}^\theta\|_{\mathcal{N}_{K_\theta}(\Omega)}^2 \leq 2a_1\lambda,$$

or

$$\left\| \delta^\theta - \hat{\delta}^\theta \right\|_n^2 + \lambda \|\hat{\delta}_{PK}^\theta\|_{\mathcal{N}_{K_\theta}(\Omega)}^2 \leq 2a_2n^{-1/2} \left\| \delta^\theta - \hat{\delta}^\theta \right\|_n^{1-\frac{d}{2m}} \left\| \hat{\delta}^\theta \right\|_{\mathcal{N}_K(\Omega)}^{d/2m}.$$

Next we consider these two cases separately.

Case I. Suppose $\left\| \delta^\theta - \hat{\delta}^\theta \right\|_n^2 + \lambda \|\hat{\delta}_{PK}^\theta\|_{\mathcal{N}_{K_\theta}(\Omega)}^2 \leq 2a_1\lambda$. Then we have

$$(A.12) \quad \begin{aligned} \left\| \delta^\theta - \hat{\delta}^\theta \right\|_n^2 &\leq 2a_1\lambda \\ \|\hat{\delta}_{PK}^\theta\|_{\mathcal{N}_{K_\theta}(\Omega)}^2 &\leq 2a_1, \end{aligned}$$

and

$$(A.13) \quad a_1\lambda \geq a_2n^{-1/2} \left\| \delta^\theta - \hat{\delta}^\theta \right\|_n^{1-\frac{d}{2m}} \left\| \hat{\delta}^\theta \right\|_{\mathcal{N}_K(\Omega)}^{d/2m}.$$

Moreover, because $\hat{\delta}^\theta \in \mathcal{N}_K(\Omega)$, then we have there is a constant $a_3 > 0$ such that

$$(A.14) \quad \|\hat{\delta}_{PK}^\theta\|_{\mathcal{N}_{K_\theta}(\Omega)}^2 \leq b_1^2 \left\| \hat{\delta}^\theta \right\|_{\mathcal{N}_K(\Omega)}^2 \leq a_3.$$

By combining (A.12)-(A.14), we have that if $\lambda \sim n^{-\frac{2m}{2m+d}}$, there are constants $a_4 > 0$ and $a_5 > 0$ such that the following inequalities hold

$$(A.15) \quad \begin{aligned} \left\| \delta^\theta - \hat{\delta}^\theta \right\|_n &\leq a_4n^{-\frac{m}{2m+d}}, \\ \|\hat{\delta}_{PK}^\theta\|_{\mathcal{N}_{K_\theta}(\Omega)} &\leq a_5. \end{aligned}$$

Case II. Suppose $\left\| \delta^\theta - \hat{\delta}^\theta \right\|_n^2 + \lambda \|\hat{\delta}_{PK}^\theta\|_{\mathcal{N}_{K_\theta}(\Omega)}^2 \leq 2a_2n^{-1/2} \left\| \delta^\theta - \hat{\delta}^\theta \right\|_n^{1-\frac{d}{2m}} \left\| \hat{\delta}^\theta \right\|_{\mathcal{N}_K(\Omega)}^{d/2m}$. Then we have

$$(A.16) \quad \begin{aligned} \left\| \delta^\theta - \hat{\delta}^\theta \right\|_n^2 &\leq 2a_2n^{-1/2} \left\| \delta^\theta - \hat{\delta}^\theta \right\|_n^{1-\frac{d}{2m}} \left\| \hat{\delta}^\theta \right\|_{\mathcal{N}_K(\Omega)}^{d/2m}, \\ \lambda \|\hat{\delta}_{PK}^\theta\|_{\mathcal{N}_{K_\theta}(\Omega)}^2 &\leq 2a_2n^{-1/2} \left\| \delta^\theta - \hat{\delta}^\theta \right\|_n^{1-\frac{d}{2m}} \left\| \hat{\delta}^\theta \right\|_{\mathcal{N}_K(\Omega)}^{d/2m}, \end{aligned}$$

and

$$(A.17) \quad a_1\lambda < a_2n^{-1/2} \left\| \delta^\theta - \hat{\delta}^\theta \right\|_n^{1-\frac{d}{2m}} \left\| \hat{\delta}^\theta \right\|_{\mathcal{N}_K(\Omega)}^{d/2m}.$$

By elementary calculations, we find that (A.16) implies

$$(A.18) \quad \begin{aligned} \left\| \delta^\theta - \hat{\delta}^\theta \right\|_n &\leq (2a_2)^{\frac{2m}{2m+d}} n^{-\frac{m}{2m+d}} \left\| \hat{\delta}^\theta \right\|_{\mathcal{N}_K(\Omega)}^{\frac{d}{2m+d}}, \\ \left\| \hat{\delta}_{PK}^\theta \right\|_{\mathcal{N}_{K_\theta}(\Omega)} &\leq (2a_2)^{\frac{2m}{2m+d}} \lambda^{-1/2} n^{-\frac{m}{2m+d}} \left\| \hat{\delta}^\theta \right\|_{\mathcal{N}_K(\Omega)}^{\frac{d}{2m+d}}. \end{aligned}$$

By combining (A.17), (A.18) and (A.14), we have that if $\lambda \sim n^{-\frac{2m}{2m+d}}$, there are constants $a_6 > 0$ and $a_7 > 0$ such that

$$(A.19) \quad \begin{aligned} \left\| \delta^\theta - \hat{\delta}^\theta \right\|_n &\leq a_6 n^{-\frac{m}{2m+d}}, \\ \left\| \hat{\delta}_{PK}^\theta \right\|_{\mathcal{N}_{K_\theta}(\Omega)} &\leq a_7. \end{aligned} \quad \blacksquare$$

The desired results then follow by combining (A.15) and (A.19).

A.4. Proof of Theorem 3.7.

Proof. The first derivative of PK loss function on $\theta_j, j = 1, \dots, q$ can be evaluated by

$$(A.20) \quad \begin{aligned} &\frac{\partial}{\partial \theta_j} \left\{ \frac{1}{n} \sum_{i=1}^n \left(\delta_i^\theta - \hat{\delta}_{PK}^\theta(\mathbf{x}_i) \right)^2 + \lambda \left\| \hat{\delta}_{PK}^\theta \right\|_{\mathcal{N}_{K_\theta}(\Omega)}^2 \right\} \\ &= \frac{2}{n} \sum_{i=1}^n \left(\delta_i^\theta - \hat{\delta}_{PK}^\theta(\mathbf{x}_i) \right) \frac{\partial \left(\delta_i^\theta - \hat{\delta}_{PK}^\theta(\mathbf{x}_i) \right)}{\partial \theta_j} + \lambda \frac{\partial \left\| \hat{\delta}_{PK}^\theta \right\|_{\mathcal{N}_{K_\theta}(\Omega)}^2}{\partial \theta_j} \end{aligned}$$

Next we consider the partial derivatives of δ_i^θ , $\hat{\delta}_{PK}^\theta$ and $\left\| \hat{\delta}_{PK}^\theta \right\|_{\mathcal{N}_{K_\theta}(\Omega)}^2$ on θ_j separately. It can be easily seen that

$$(A.21) \quad \frac{\partial \delta_i^\theta}{\partial \theta_j} = -\frac{\partial y^s(\mathbf{x}_i, \boldsymbol{\theta})}{\partial \theta_j}.$$

From Proposition 3.2, $\hat{\delta}_{PK}^\theta = \hat{\delta}^\theta - \mathcal{P}_{\mathcal{G}_\theta} \hat{\delta}^\theta$. Because $\mathcal{P}_{\mathcal{G}_\theta} \hat{\delta}^\theta = \mathbf{b}_\theta^T \mathbf{E}_\theta^{-1} \mathbf{g}_\theta$, where $\mathbf{g}_\theta^T(\cdot) = \frac{\partial y^s(\cdot, \boldsymbol{\theta})}{\partial \boldsymbol{\theta}} = \left(\frac{\partial y^s(\cdot, \boldsymbol{\theta})}{\partial \theta_1}, \dots, \frac{\partial y^s(\cdot, \boldsymbol{\theta})}{\partial \theta_q} \right)$ and $\mathbf{b}_\theta^T = \int_{\Omega} \hat{\delta}^\theta(\mathbf{x}) \frac{\partial y^s(\mathbf{x}, \boldsymbol{\theta})}{\partial \boldsymbol{\theta}} d\mathbf{x}$, by some elementary calculations, we have that

$$(A.22) \quad \frac{\partial \hat{\delta}_{PK}^\theta}{\partial \theta_j} = -\frac{\partial y^s(\mathbf{x}_i, \boldsymbol{\theta})}{\partial \theta_j} - \frac{\partial \mathbf{b}_\theta^T}{\partial \theta_j} \mathbf{E}_\theta^{-1} \mathbf{g}_\theta - \mathbf{b}_\theta^T \frac{\partial \mathbf{E}_\theta^{-1}}{\partial \theta_j} \mathbf{g}_\theta - \mathbf{b}_\theta^T \mathbf{E}_\theta^{-1} \frac{\partial \mathbf{g}_\theta}{\partial \theta_j}.$$

It following from Lemma 6.6 of [24] that

$$(A.23) \quad \frac{\partial \left\| \hat{\delta}_{PK}^\theta \right\|_{\mathcal{N}_{K_\theta}(\Omega)}^2}{\partial \theta_j} = O_p(1).$$

Plugging (A.21) -(A.23) into (A.20), and also since $\lambda \sim n^{-\frac{2m}{2m+d}}$ holds, we have that the partial derivative of the PK loss function becomes

$$\begin{aligned}
& \frac{2}{n} \sum_{i=1}^n \left(\delta_i^\theta - \hat{\delta}_{PK}^\theta(\mathbf{x}_i) \right) \frac{\partial \left(\delta_i^\theta - \hat{\delta}_{PK}^\theta(\mathbf{x}_i) \right)}{\partial \theta_j} + o_p(n^{-1/2}) \\
\text{(A.24)} \quad &= \frac{\partial \mathbf{b}_\theta^T}{\partial \theta_j} \mathbf{E}_\theta^{-1} \frac{2}{n} \sum_{i=1}^n \delta_i^\theta \mathbf{g}_\theta(\mathbf{x}_i) + \mathbf{b}_\theta^T \frac{\partial \mathbf{E}_\theta^{-1}}{\partial \theta_j} \frac{2}{n} \sum_{i=1}^n \delta_i^\theta \mathbf{g}_\theta(\mathbf{x}_i) + \mathbf{b}_\theta^T \mathbf{E}_\theta^{-1} \frac{2}{n} \sum_{i=1}^n \delta_i^\theta \frac{\partial \mathbf{g}_\theta(\mathbf{x}_i)}{\partial \theta_j} \\
& \quad - \mathbf{b}_\theta^T \mathbf{E}_\theta^{-1} \frac{2}{n} \sum_{i=1}^n \hat{\delta}_{PK}^\theta(\mathbf{x}_i) \frac{\partial \mathbf{g}_\theta(\mathbf{x}_i)}{\partial \theta_j} + o_p(n^{-1/2}).
\end{aligned}$$

Then we work on $\frac{1}{n} \sum_{i=1}^n \delta_i^\theta \mathbf{g}_\theta(\mathbf{x}_i)$, $\frac{1}{n} \sum_{i=1}^n \delta_i^\theta \frac{\partial \mathbf{g}_\theta(\mathbf{x}_i)}{\partial \theta_j}$ and $\frac{2}{n} \sum_{i=1}^n \hat{\delta}_{PK}^\theta(\mathbf{x}_i) \frac{\partial \mathbf{g}_\theta(\mathbf{x}_i)}{\partial \theta_j}$ separately. By the definition of δ_i^θ , it is easily obtained that

$$\text{(A.25)} \quad \frac{1}{n} \sum_{i=1}^n \delta_i^\theta \mathbf{g}_\theta(\mathbf{x}_i) = \langle \delta^\theta, \mathbf{g}_\theta \rangle_n + \langle \epsilon, \mathbf{g}_\theta \rangle_n.$$

Because $\mathcal{N}_{K_\theta}(\Omega)$ can be continuously embedded into the Sobolev space $H^m(\Omega)$, it follows from Theorem 5.11 of [28] that $\frac{1}{\sqrt{n}} \sum_{i=1}^n \epsilon_i \mathbf{g}_\theta(\mathbf{x}_i) = O_p(1)$. By combining with (A.7), we have

$$\text{(A.26)} \quad \frac{1}{n} \sum_{i=1}^n \delta_i^\theta \mathbf{g}_\theta(\mathbf{x}_i) = \langle \delta^\theta, \mathbf{g}_\theta \rangle_{L_2(\Omega)} + O_p(n^{-1/2}).$$

Similarly,

$$\begin{aligned}
\text{(A.27)} \quad & \frac{1}{n} \sum_{i=1}^n \delta_i^\theta \frac{\partial \mathbf{g}_\theta(\mathbf{x}_i)}{\partial \theta_j} = \langle \delta^\theta, \frac{\partial \mathbf{g}_\theta(\mathbf{x}_i)}{\partial \theta_j} \rangle_n + \langle \epsilon, \frac{\partial \mathbf{g}_\theta(\mathbf{x}_i)}{\partial \theta_j} \rangle_n, \\
& = \frac{\partial \langle \delta^\theta, \mathbf{g}_\theta \rangle_{L_2(\Omega)}}{\partial \theta_j} + \int \frac{\partial y^s(\mathbf{x}, \boldsymbol{\theta})}{\partial \theta_j} \mathbf{g}_\theta d\mathbf{x} + O_p(n^{-\frac{1}{2}}).
\end{aligned}$$

Because $\int \hat{\delta}_{PK}^\theta \mathbf{g}_\theta d\mathbf{x} = 0$, taking the partial derivative of $\int \hat{\delta}_{PK}^\theta \mathbf{g}_\theta d\mathbf{x}$ on θ_j , we have

$$\int \frac{\partial \hat{\delta}_{PK}^\theta}{\partial \theta_j} \mathbf{g}_\theta d\mathbf{x} + \int \hat{\delta}_{PK}^\theta \frac{\partial \mathbf{g}_\theta}{\partial \theta_j} d\mathbf{x} = 0.$$

Moverover, because $\int \mathbf{g}_\theta \mathbf{g}_\theta^T d\mathbf{x} = \mathbf{E}_\theta$, and $\frac{\partial \mathbf{E}_\theta^{-1}}{\partial \theta_j} = -\mathbf{E}_\theta^{-1} \frac{\partial \mathbf{E}_\theta}{\partial \theta_j} \mathbf{E}_\theta^{-1}$, we have

$$\begin{aligned}
\text{(A.28)} \quad & \int \hat{\delta}_{PK}^\theta \frac{\partial \mathbf{g}_\theta}{\partial \theta_j} d\mathbf{x} = - \int \mathbf{g}_\theta \frac{\partial \hat{\delta}_{PK}^\theta}{\partial \theta_j} d\mathbf{x}, \\
& = \int \mathbf{g}_\theta \frac{\partial y^s(\mathbf{x}_i, \boldsymbol{\theta})}{\partial \theta_j} d\mathbf{x} + \frac{\partial \mathbf{b}_\theta}{\partial \theta_j} + \frac{1}{2} \mathbf{E}_\theta \frac{\partial \mathbf{E}_\theta^{-1}}{\partial \theta_j} \mathbf{b}_\theta.
\end{aligned}$$

By combining (A.26), (A.27) and (A.28), we have that (A.24) can be represented as

$$\text{(A.29)} \quad 2 \frac{\partial \mathbf{b}_\theta^T}{\partial \theta_j} \mathbf{E}_\theta^{-1} (\boldsymbol{\alpha}_\theta - \mathbf{b}_\theta) + 2 \frac{\partial \boldsymbol{\alpha}_\theta^T}{\partial \theta_j} \mathbf{E}_\theta^{-1} \mathbf{b}_\theta + \boldsymbol{\alpha}_\theta^T \frac{\partial \mathbf{E}_\theta^{-1}}{\partial \theta_j} (2\boldsymbol{\alpha}_\theta - \mathbf{b}_\theta) + O_p(n^{-\frac{1}{2}}).$$

Let $\mathbf{a}_{\theta^s} = \mathbf{0}$, to check whether θ^s is a local maximum or a local minimum of the PPK loss function, the Hessian matrix of $L_{PK}(\theta)$ at θ^s , denotes as $\mathbf{H}_{PK}(\theta^s)$, can be evaluated from (A.29). Following from the Proposition 3.4, together with the Cauchy-Schwarz inequality, we have that $\mathbf{b}_\theta = \mathbf{a}_\theta + O_p(n^{-\frac{m}{2m+d}})$, and thus

$$(A.30) \quad \mathbf{H}_{PK}(\theta^s) = 2 \frac{\partial \mathbf{a}_{\theta^s}^T}{\partial \theta} \mathbf{E}_{\theta^s}^{-1} \frac{\partial \mathbf{a}_{\theta^s}^T}{\partial \theta} + O_p(n^{-\frac{m}{2m+d}}).$$

That is, the desired results are obtained. ■

Appendix B. Technical proofs in Section 4. In this section, we prove the theorems in Section 4.

B.1. Proof of Theorem 4.1 .

Proof. From (4.2), the stationary points of PPK loss function satisfy that

$$(B.1) \quad 0 = \frac{\partial}{\partial \theta_j} \left\{ L_{PK}(\theta) + \eta \|\hat{\delta}_{PK}^\theta\|_{L_2(\Omega)}^2 \right\}.$$

The partial derivative of $\|\hat{\delta}_{PK}^\theta\|_{L_2(\Omega)}^2$ on θ_j is

$$(B.2) \quad \frac{\partial \|\hat{\delta}_{PK}^\theta\|_{L_2(\Omega)}^2}{\partial \theta_j} = \frac{\partial \int_{\Omega} (\hat{\delta}_{PK}^\theta)^2 dx}{\partial \theta_j} = 2 \int_{\Omega} \hat{\delta}_{PK}^\theta \frac{\partial \hat{\delta}_{PK}^\theta}{\partial \theta_j} dx.$$

where $\frac{\partial \hat{\delta}_{PK}^\theta}{\partial \theta_j}$ is shown in (A.22). Because $\int \hat{\delta}_{PK}^\theta \mathbf{g}_\theta dx = \mathbf{0}$,

$$(B.3) \quad \begin{aligned} 2 \int_{\Omega} \hat{\delta}_{PK}^\theta \frac{\partial \hat{\delta}_{PK}^\theta}{\partial \theta_j} dx &= 2 \int_{\Omega} \hat{\delta}_{PK}^\theta \times \left(-\frac{\partial y^s(\mathbf{x}, \theta)}{\partial \theta_j} - \frac{\partial \mathbf{b}_\theta^T}{\partial \theta_j} \mathbf{E}_\theta^{-1} \mathbf{g}_\theta - \mathbf{b}_\theta^T \frac{\partial \mathbf{E}_\theta^{-1}}{\partial \theta_j} \mathbf{g}_\theta - \mathbf{b}_\theta^T \mathbf{E}_\theta^{-1} \frac{\partial \mathbf{g}_\theta}{\partial \theta_j} \right) dx, \\ &= -2 \mathbf{b}_\theta^T \mathbf{E}_\theta^{-1} \int_{\Omega} \hat{\delta}_{PK}^\theta \frac{\partial \mathbf{g}_\theta}{\partial \theta_j} dx. \end{aligned}$$

The integration by parts formula suggests that $\frac{\partial \mathbf{b}_\theta}{\partial \theta_j} = \int_{\Omega} \hat{\delta}_{PK}^\theta \frac{\partial \mathbf{g}_\theta}{\partial \theta_j} dx - \int_{\Omega} \frac{\partial y^s(\mathbf{x}, \theta)}{\partial \theta_j} \mathbf{g}_\theta dx$, and $\frac{\partial \mathbf{E}_\theta}{\partial \theta_j} = 2 \int \frac{\partial \mathbf{g}_\theta}{\partial \theta_j} \mathbf{g}_\theta^T dx$. The derivative of inverse matrix shows that $\frac{\partial \mathbf{E}_\theta^{-1}}{\partial \theta_j} = -\mathbf{E}_\theta^{-1} \frac{\partial \mathbf{E}_\theta}{\partial \theta_j} \mathbf{E}_\theta^{-1}$. Thus we have

$$(B.4) \quad 2 \int_{\Omega} \hat{\delta}_{PK}^\theta \frac{\partial \mathbf{g}_\theta}{\partial \theta_j} dx = -2 \mathbf{b}_\theta^T \mathbf{E}_\theta^{-1} \frac{\partial \mathbf{b}_\theta}{\partial \theta_j} - 2 \mathbf{b}_\theta^T \mathbf{E}_\theta^{-1} \int_{\Omega} \frac{\partial y^s(\mathbf{x}, \theta)}{\partial \theta_j} \mathbf{g}_\theta dx - \mathbf{b}_\theta^T \frac{\partial \mathbf{E}_\theta^{-1}}{\partial \theta_j} \mathbf{b}_\theta.$$

Combining (A.26), (A.27) and (A.28), we have that (B.1) can be represented as

$$(B.5) \quad (1 - \eta) \left[2 \frac{\partial \mathbf{a}_\theta^T}{\partial \theta_j} \mathbf{E}_\theta^{-1} \mathbf{a}_\theta + \mathbf{a}_\theta^T \frac{\partial \mathbf{E}_\theta^{-1}}{\partial \theta_j} \mathbf{a}_\theta \right] - 2 \eta \mathbf{a}_\theta^T \mathbf{E}_\theta^{-1} \int_{\Omega} \frac{\partial y^s(\mathbf{x}, \theta)}{\partial \theta_j} \mathbf{g}_\theta dx + O_p(n^{-\frac{m}{2m+d}}).$$

Now we compare η with 1, and consider two different cases.

Case I. If $\eta = 1$, because $\mathbf{E}_\theta = \int \mathbf{g}_\theta \mathbf{g}_\theta^T d\mathbf{x}$. then we have

$$(B.6) \quad \frac{\partial}{\partial \boldsymbol{\theta}} \left\{ L_{PK}(\boldsymbol{\theta}) + \eta \|\hat{\delta}_{PK}^\theta\|_{L_2(\Omega)}^2 \right\} = -2\mathbf{a}_\theta^T + O_p(n^{-\frac{m}{2m+d}}).$$

Recall that $\boldsymbol{\theta}^s$ is a stationary point of the L_2 loss function, which satisfy that,

$$(B.7) \quad \int (\zeta(\mathbf{x}) - y^s(\mathbf{x}, \boldsymbol{\theta}^s)) \frac{\partial y^s(\mathbf{x}, \boldsymbol{\theta}^s)}{\partial \boldsymbol{\theta}} d\mathbf{x} = \mathbf{a}_{\boldsymbol{\theta}^s}^T = \mathbf{0}.$$

We have $\boldsymbol{\theta}^s$ is a stationary point of the PPK loss function. The Hessian matrix at $\boldsymbol{\theta}^s$ can easily obtained by evaluating second derivative of the PPK loss on $\boldsymbol{\theta}$,

$$(B.8) \quad \frac{\partial^2}{\partial \boldsymbol{\theta} \partial \boldsymbol{\theta}^T} \left\{ L_{PK}(\boldsymbol{\theta}) + \eta \|\hat{\delta}_{PK}^\theta\|_{L_2(\Omega)}^2 \right\} |_{\boldsymbol{\theta}=\boldsymbol{\theta}^s} = -2 \left(\frac{\partial \mathbf{a}_\theta}{\partial \boldsymbol{\theta}} \right)^T |_{\boldsymbol{\theta}=\boldsymbol{\theta}^s} + O_p(n^{-\frac{m}{2m+d}}).$$

Moreover, Hessian matrix at $\boldsymbol{\theta}^s$ of the L_2 loss function is

$$(B.9) \quad \frac{\partial^2}{\partial \boldsymbol{\theta} \partial \boldsymbol{\theta}^T} \left\{ \|\zeta(\cdot) - y^s(\cdot, \boldsymbol{\theta})\|_{L_2(\Omega)}^2 \right\} |_{\boldsymbol{\theta}=\boldsymbol{\theta}^s} = -2 \left(\frac{\partial \mathbf{a}_\theta}{\partial \boldsymbol{\theta}} \right)^T.$$

It is easily to be proven that, $\frac{\partial \mathbf{a}_\theta}{\partial \boldsymbol{\theta}} = \lim_{n \rightarrow \infty} \frac{\partial \mathbf{b}_\theta}{\partial \boldsymbol{\theta}}$. By the order-preserving propertie of limits of real sequences, we have that if $\boldsymbol{\theta}^s$ is a local minimum (maximum) of the L_2 loss function, then $\boldsymbol{\theta}^s$ is a local minimum (maximum) of the PPK loss function.

Case II. If $\eta \neq 1$, then

$$(B.10) \quad \begin{aligned} & \frac{\partial^2}{\partial \boldsymbol{\theta} \partial \boldsymbol{\theta}^T} \left\{ L_{PK}(\boldsymbol{\theta}) + \eta \|\hat{\delta}_{PK}^\theta\|_{L_2(\Omega)}^2 \right\} |_{\boldsymbol{\theta}=\boldsymbol{\theta}^s} \\ &= (1 - \eta) \left(\frac{\partial \mathbf{a}_\theta}{\partial \boldsymbol{\theta}} \right)^T \mathbf{E}_\theta^{-1} \frac{\partial \mathbf{a}_\theta}{\partial \boldsymbol{\theta}} |_{\boldsymbol{\theta}=\boldsymbol{\theta}^s} - 2\eta \left(\frac{\partial \mathbf{a}_\theta}{\partial \boldsymbol{\theta}} \right)^T |_{\boldsymbol{\theta}=\boldsymbol{\theta}^s} + O_p(n^{-\frac{m}{2m+d}}), \\ &= (1 - \eta) \left(\frac{\partial \mathbf{a}_\theta}{\partial \boldsymbol{\theta}} \right)^T |_{\boldsymbol{\theta}=\boldsymbol{\theta}^s} \mathbf{E}_{\boldsymbol{\theta}^s}^{-1} \left\{ \frac{\partial \mathbf{a}_\theta}{\partial \boldsymbol{\theta}} - 2\eta/(1 - \eta)\mathbf{E}_\theta \right\} |_{\boldsymbol{\theta}=\boldsymbol{\theta}^s} + O_p(n^{-\frac{m}{2m+d}}), \end{aligned}$$

Now, we want to find the interval of η such that if $\frac{\partial \mathbf{a}_\theta}{\partial \boldsymbol{\theta}} |_{\boldsymbol{\theta}=\boldsymbol{\theta}^s}$ is positive (negative) definite, then $\frac{\partial^2}{\partial \boldsymbol{\theta} \partial \boldsymbol{\theta}^T} \{L_{PPK}(\boldsymbol{\theta})\} |_{\boldsymbol{\theta}=\boldsymbol{\theta}^s}$ is negative (positive) definite. That is, the product of $(1 - \eta)$ and $\left\{ \frac{\partial \mathbf{a}_\theta}{\partial \boldsymbol{\theta}} - 2\eta/(1 - \eta)\mathbf{E}_\theta \right\} |_{\boldsymbol{\theta}=\boldsymbol{\theta}^s}$ is negative definite.

Suppose there exist constants $U \geq L$, such that

$$U\mathbf{E}_{\boldsymbol{\theta}^s} > \frac{\partial \mathbf{a}_\theta}{\partial \boldsymbol{\theta}} |_{\boldsymbol{\theta}=\boldsymbol{\theta}^s} > L\mathbf{E}_{\boldsymbol{\theta}^s}.$$

Then we have

$$(B.11) \quad \left(U - \frac{2\eta}{1 - \eta} \right) \mathbf{E}_\theta > \left\{ \frac{\partial \mathbf{b}_\theta}{\partial \boldsymbol{\theta}} - \frac{2\eta}{1 - \eta} \mathbf{E}_\theta \right\} |_{\boldsymbol{\theta}=\boldsymbol{\theta}^s} > \left(L - \frac{2\eta}{1 - \eta} \right) \mathbf{E}_\theta.$$

To evaluating the production of $1 - \eta$ and (B.11), We consider the sign of $1 - \eta$.

(A) If $(1 - \eta) > 0$, then $(U - \frac{2\eta}{1-\eta}) < 0$ is needed to guarantee that $\frac{\partial^2}{\partial\theta\partial\theta^T} \{L_{PPK}(\boldsymbol{\theta})\} |_{\boldsymbol{\theta}=\boldsymbol{\theta}^s}$ is negative definite. That is $U < (U + 2)\eta$ and $\eta < 1$.

(B) If $(1 - \eta) < 0$, then $(L - \frac{2\eta}{1-\eta}) > 0$ is needed. That is $L < (L + 2)\eta$ and $\eta > 1$.

By combining Case I and Case II, we have η belongs to the set $\Gamma_\eta = \{\eta = 1\} \cup \{U < (U+2)\eta \text{ and } \eta < 1\} \cup \{L < (L+2)\eta \text{ and } \eta > 1\}$. By some easy calculations, Γ_η can be represented as

$$(B.12) \quad \Gamma_\eta = \begin{cases} 0 \leq \eta < \frac{L}{L+2} & L < U \leq -2 \text{ or } L = U < -2 \\ \max(0, \frac{U}{U+2}) < \eta < \frac{L}{L+2} & L < -2 < U \\ \eta > \max(0, \frac{U}{U+2}) & -2 \leq L < U \text{ or } L = U > -2 \\ \eta \geq 0 & L = U = -2 \end{cases} \quad \blacksquare$$

B.2. Proof of Theorem 4.2.

Proof. We first prove that $\hat{\boldsymbol{\theta}}_{PPK}$ converges to $\boldsymbol{\theta}^*$ in probability. The desired results can be proved by showing that

$$(B.13) \quad L_{PPK}(\boldsymbol{\theta}^*) \leq \inf_{\|\boldsymbol{\theta}-\boldsymbol{\theta}^*\|=cn^{-\frac{m}{2m+d}}} L_{PPK}(\boldsymbol{\theta}),$$

for sufficiently large n and some constant $c > 0$ to be specified later, where $\|\cdot\|$ denotes the usual Euclidean distance. Then we prove that $\hat{\boldsymbol{\theta}}_{PPK}$ converges in distribution to a normal distribution by following the standard framework for establishing asymptotic theory for M-estimation.

We use the converse method to prove that (B.13) holds. Suppose (B.13) is false. Then there exists $\tilde{\boldsymbol{\theta}}$ with $\|\boldsymbol{\theta}^* - \tilde{\boldsymbol{\theta}}\| = cn^{-\frac{m}{2m+d}}$ so that

$$(B.14) \quad L_{PK}(\boldsymbol{\theta}^*) + \eta \|\hat{\delta}_{PK}^{\boldsymbol{\theta}^*}\|_{L_2(\Omega)}^2 > L_{PK}(\tilde{\boldsymbol{\theta}}) + \eta \|\hat{\delta}_{PK}^{\tilde{\boldsymbol{\theta}}}\|_{L_2(\Omega)}^2.$$

Because the sequence $\{\hat{\boldsymbol{\theta}}_{PK}\}$ converges to $\boldsymbol{\theta}^*$ in probability as n goes to infinity. By the proof of Theorem 4.2 in [24], we have that

$$(B.15) \quad L_{PK}(\boldsymbol{\theta}^*) \leq \inf_{\|\boldsymbol{\theta}-\boldsymbol{\theta}^*\|=c_1n^{-\frac{m}{2m+d}}} L_{PK}(\boldsymbol{\theta}),$$

for sufficiently large n and some constant $c_1 > 0$. Let $c = c_1$, (B.15) implies that

$$(B.16) \quad L_{PK}(\boldsymbol{\theta}^*) \leq L_{PK}(\tilde{\boldsymbol{\theta}}).$$

Combining (B.14) and (B.16), we arrive at

$$(B.17) \quad \|\hat{\delta}_{PK}^{\boldsymbol{\theta}^*}\|_{L_2(\Omega)}^2 > \|\hat{\delta}_{PK}^{\tilde{\boldsymbol{\theta}}}\|_{L_2(\Omega)}^2.$$

On the other hand, by the definition of $\boldsymbol{\theta}^*$,

$$(B.18) \quad \|\delta^{\boldsymbol{\theta}^*}\|_{L_2(\Omega)}^2 \leq \|\delta^{\tilde{\boldsymbol{\theta}}}\|_{L_2(\Omega)}^2.$$

By the uniform convergence $\hat{\delta}_{PK}^\theta$ in Proposition 3.4, we have

$$(B.19) \quad \lim_{n \rightarrow \infty} \|\hat{\delta}_{PK}^{\theta^*}\|_{L_2(\Omega)}^2 = \|\delta^{\theta^*}\|_{L_2(\Omega)}^2.$$

By the order-preserving properties of limits of real sequences, there exist $N \in \mathbf{R}$ such that, for any $n > N$,

$$(B.20) \quad \|\hat{\delta}_{PK}^{\theta^*}\|_{L_2(\Omega)}^2 \leq \|\hat{\delta}_{PK}^{\tilde{\theta}}\|_{L_2(\Omega)}^2.$$

This leads to a contradiction.

Next we prove that $\hat{\boldsymbol{\theta}}_{PPK}$ converges in distribution to a normal distribution. Because $\hat{\delta}_{PK}^{\hat{\boldsymbol{\theta}}_{PPK}} = \mathcal{P}_{\hat{\mathcal{G}}_{\hat{\boldsymbol{\theta}}_{PPK}}}^\perp \hat{\delta}^{\hat{\boldsymbol{\theta}}_{PPK}}$, by the definition of $\hat{\boldsymbol{\theta}}_{PPK}$, we have

$$(B.21) \quad \frac{\partial \tilde{l}(\boldsymbol{\theta})}{\partial \boldsymbol{\theta}} \Big|_{\boldsymbol{\theta}=\hat{\boldsymbol{\theta}}_{PPK}} = 0,$$

where

$$\tilde{l}(\boldsymbol{\theta}) = \frac{1}{n} \sum_{i=1}^n \left(y_i - y^s(\mathbf{x}_i, \boldsymbol{\theta}) - \mathcal{P}_{\hat{\mathcal{G}}_\theta}^\perp \hat{\delta}^{\hat{\boldsymbol{\theta}}_{PPK}}(\mathbf{x}_i) \right)^2 + \lambda \|\mathcal{P}_{\hat{\mathcal{G}}_\theta}^\perp \hat{\delta}^{\hat{\boldsymbol{\theta}}_{PPK}}\|_{\mathcal{N}_{K_\theta}(\Omega)}^2 + \eta \|\mathcal{P}_{\hat{\mathcal{G}}_\theta}^\perp \hat{\delta}^{\hat{\boldsymbol{\theta}}_{PPK}}\|_{L_2(\Omega)}^2.$$

Involved with $\mathcal{P}_{\hat{\mathcal{G}}_\theta} \hat{\delta}^{\hat{\boldsymbol{\theta}}_{PPK}} = \tilde{\mathbf{b}}_\theta^T \mathbf{E}_\theta^{-1} \mathbf{g}_\theta$, where $\tilde{\mathbf{b}}_\theta = \langle \hat{\delta}^{\hat{\boldsymbol{\theta}}_{PPK}}, \mathbf{g}_\theta \rangle_{L_2(\Omega)}$, we have that

$$\frac{\partial \mathcal{P}_{\hat{\mathcal{G}}_\theta}^\perp \hat{\delta}^{\hat{\boldsymbol{\theta}}_{PPK}}}{\partial \boldsymbol{\theta}} = -\frac{\partial \tilde{\mathbf{b}}_\theta^T}{\partial \boldsymbol{\theta}} \mathbf{E}_\theta^{-1} \mathbf{g}_\theta - \tilde{\mathbf{b}}_\theta^T \frac{\partial \mathbf{E}_\theta^{-1} \mathbf{g}_\theta}{\partial \boldsymbol{\theta}}.$$

Because $\langle \mathcal{P}_{\hat{\mathcal{G}}_\theta}^\perp \hat{\delta}^{\hat{\boldsymbol{\theta}}_{PPK}}, \mathbf{g}_\theta \rangle \Big|_{\boldsymbol{\theta}=\hat{\boldsymbol{\theta}}_{PPK}} = \mathbf{0}$, we can easily verify that

$$\frac{\partial \mathcal{P}_{\hat{\mathcal{G}}_\theta}^\perp \hat{\delta}^{\hat{\boldsymbol{\theta}}_{PPK}}}{\partial \boldsymbol{\theta}} \Big|_{\boldsymbol{\theta}=\hat{\boldsymbol{\theta}}_{PPK}} = -\frac{\partial \tilde{\mathbf{b}}_\theta^T}{\partial \boldsymbol{\theta}} \mathbf{E}_\theta^{-1} \mathbf{g}_\theta \Big|_{\boldsymbol{\theta}=\hat{\boldsymbol{\theta}}_{PPK}},$$

and

$$\frac{\partial \|\mathcal{P}_{\hat{\mathcal{G}}_\theta}^\perp \hat{\delta}^{\hat{\boldsymbol{\theta}}_{PPK}}\|_{L_2(\Omega)}^2}{\partial \boldsymbol{\theta}} \Big|_{\boldsymbol{\theta}=\hat{\boldsymbol{\theta}}_{PPK}} = \mathbf{0}.$$

Moreover, Eq. (69) in [24] shows that

$$\lambda \frac{\partial \|\mathcal{P}_{\hat{\mathcal{G}}_\theta}^\perp \hat{\delta}^{\hat{\boldsymbol{\theta}}_{PPK}}\|_{\mathcal{N}_{K_\theta}(\Omega)}^2}{\partial \boldsymbol{\theta}} \Big|_{\boldsymbol{\theta}=\hat{\boldsymbol{\theta}}_{PPK}} = o_p(n^{-1/2}).$$

By some elementary calculations, (B.21) becomes

$$(B.22) \quad \frac{1}{n} \sum_{i=1}^n \left[(\zeta(\mathbf{x}_i) - y^s(\mathbf{x}_i, \hat{\boldsymbol{\theta}}_{PPK})) \mathbf{g}_{\hat{\boldsymbol{\theta}}_{PPK}} \right] + \frac{1}{n} \sum_{i=1}^n \epsilon_i \mathbf{g}_{\hat{\boldsymbol{\theta}}_{PPK}} = o_p(n^{-1/2}).$$

By applying Taylor's theorem, the first part of (B.22) can be represented by

$$(B.23) \quad \frac{1}{n} \sum_{i=1}^n [(\zeta(\mathbf{x}_i) - y^s(\mathbf{x}_i, \boldsymbol{\theta}^*)) \mathbf{g}_{\boldsymbol{\theta}^*}] - \frac{1}{2} \mathbf{V}(\hat{\boldsymbol{\theta}}_{PPK} - \boldsymbol{\theta}^*) + o_p(n^{-1/2}).$$

Because $\delta^* = \delta^{\boldsymbol{\theta}^*} \in \mathcal{G}_{\boldsymbol{\theta}^*}^\perp$, together with the asymptotic equivalence relation between the L_2 and the empirical norm (A.7), there is $\frac{1}{n} \sum_{i=1}^n [(\zeta(\mathbf{x}_i) - y^s(\mathbf{x}_i, \boldsymbol{\theta}^*)) \mathbf{g}_{\boldsymbol{\theta}^*}] = o_p(n^{-1/2})$. The desired result can be then obtained by combining (B.22) and (B.23). \blacksquare

B.3. Proof of Theorem 4.3.

Proof. Let $\hat{\zeta}_n(\cdot) = \hat{\delta}_{PK}^{\hat{\theta}^{PPK}}(\cdot) + y^s(\cdot, \hat{\theta}_{PPK})$, which is an estimator of $\zeta(\cdot)$. The triangle inequality implies that

$$(B.24) \quad \begin{aligned} \|\hat{\zeta}_n - \zeta\|_{L_2(\Omega)} &\leq \|\hat{\delta}_{PK}^{\theta^*} - \delta^*\|_{L_2(\Omega)} + \\ &\|\hat{\delta}_{PK}^{\hat{\theta}^{PPK}} - \hat{\delta}_{PK}^{\theta^*}\|_{L_2(\Omega)} + \|y^s(\cdot, \hat{\theta}_{PPK}) - y^s(\cdot, \theta^*)\|_{L_2(\Omega)}, \\ &= \text{I} + \text{II} + \text{III}. \end{aligned}$$

Next we bound (I), (II) and (III) respectively.

For (I), because $\delta^* = \delta^{\theta^*} \in \mathcal{G}_{\theta^*}^\perp$, it follows from Corollary 3.6 that

$$\text{I} \leq \sup_{\theta \in \Theta} \left\| \mathcal{P}_{\mathcal{G}_\theta}^\perp \delta^\theta - \hat{\delta}_{PK}^\theta \right\|_{L_2(\Omega)} = O_p(n^{-\frac{m}{2m+d}}).$$

For (II), we can apply Taylor's theorem to conclude that

$$(B.25) \quad \|\hat{\delta}_{PK}^{\hat{\theta}^{PPK}} - \hat{\delta}_{PK}^{\theta^*}\|_{L_2(\Omega)} \leq \left\| \frac{\partial \hat{\delta}_{PK}^{\theta^*}}{\partial \theta} \right\|_{L_2(\Omega)} \|\hat{\theta}_{PPK} - \theta^*\| + O_p(\|\hat{\theta}_{PPK} - \theta^*\|^2).$$

Here, $\|\cdot\|$ is the euclidean distance. The first derivative of $\hat{\delta}_{PK}^\theta$ on $\theta_j, j = 1, \dots, q$ (A.22) suggests that

$$(B.26) \quad \begin{aligned} \frac{\partial \hat{\delta}_{PK}^\theta}{\partial \theta_j} |_{\theta^*} &= -\frac{\partial y^s(\mathbf{x}, \theta^*)}{\partial \theta_j} - \frac{\partial \mathbf{b}_{\theta^*}^T}{\partial \theta_j} \mathbf{E}_{\theta^*}^{-1} \mathbf{g}_{\theta^*}(\mathbf{x}) - \mathbf{b}_{\theta^*}^T \frac{\partial \mathbf{E}_{\theta^*}^{-1}}{\partial \theta_j} \mathbf{g}_{\theta^*}(\mathbf{x}) - \mathbf{b}_{\theta^*}^T \mathbf{E}_{\theta^*}^{-1} \frac{\partial \mathbf{g}_{\theta^*}(\mathbf{x})}{\partial \theta_j}, \\ &= -\langle \delta^*, \frac{\partial^2 y^s(\mathbf{x}, \theta^*)}{\partial \theta_i \partial \theta_j} \rangle_{L_2(\Omega)} \mathbf{E}_{\theta^*}^{-1} \mathbf{g}_{\theta^*}(\mathbf{x}) + O_p(n^{-\frac{m}{2m+d}}). \end{aligned}$$

The last equality is following from Proposition 3.4. By condition A3 and condition B2, together with the triangle inequality, we have that $\left\| \frac{\partial \hat{\delta}_{PK}^{\theta^*}}{\partial \theta_j} \right\|_{L_2(\Omega)}$ can be bounded by a finite constant.

Combining with the asymptotic normal of $\hat{\theta}_{PPK}$, we have that $\text{II} = O_p(n^{-1/2})$.

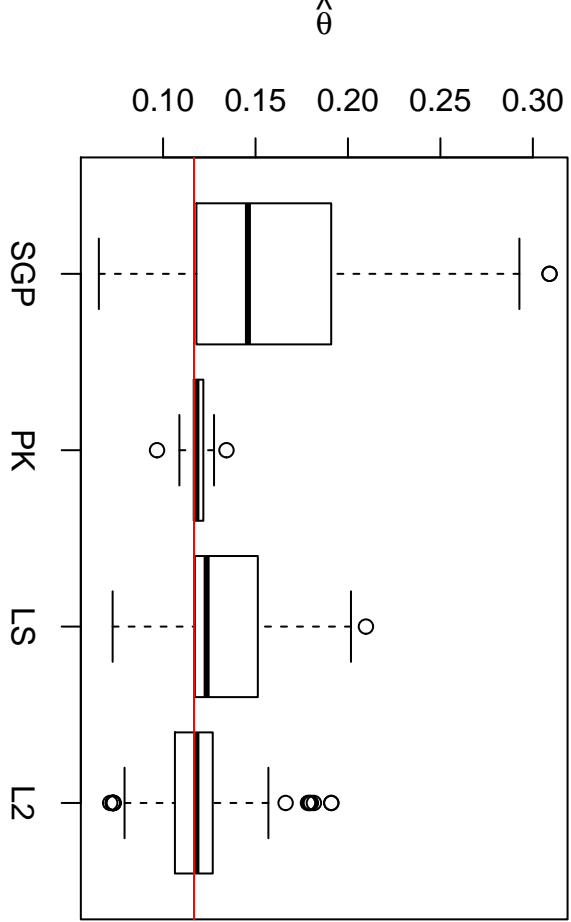
Following a similar argument, we have $\text{III} = O_p(n^{-1/2})$. This leads to the desired result.

REFERENCES

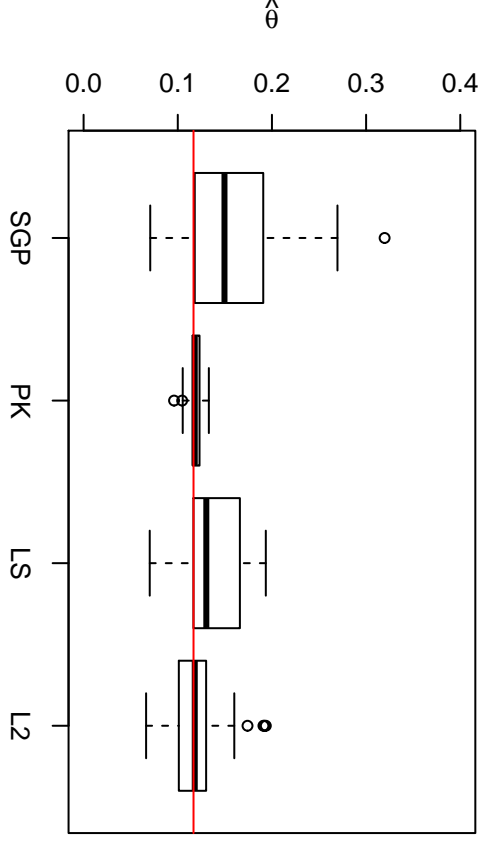
- [1] M. J. BAYARRI, J. O. BERGER, R. PAULO, J. SACKS, J. A. CAFEO, J. CAVENDISH, C.-H. LIN, AND J. TU, *A framework for validation of computer models*, Technometrics, 49 (2007).
- [2] N. L. CAROTHERS, *Real analysis*, Cambridge University Press, 2000.
- [3] M. GU, J. PALOMO, AND J. O. BERGER, *Robustgasp: Robust Gaussian stochastic process emulation in R*, arXiv preprint arXiv:1801.01874, (2018).
- [4] M. GU AND L. WANG, *Scaled Gaussian stochastic process for computer model calibration and prediction*, SIAM/ASA Journal on Uncertainty Quantification, 6 (2018), pp. 1555–1583.
- [5] M. GU, F. XIE, AND L. WANG, *A theoretical framework of the scaled Gaussian stochastic process in prediction and calibration*, arXiv preprint arXiv:1807.03829, (2018).
- [6] F. GÜRBÜZ, *Some estimates for generalized commutators of rough fractional maximal and integral operators on generalized weighted Morrey spaces*, Canadian Mathematical Bulletin, 60 (2017), pp. 131–145.

- [7] F. GÜRBÜZ, *Generalized local Morrey spaces and multilinear commutators generated by marcinkiewicz integrals with rough kernel associated with schrödinger operators and local campanato functions*, Journal of Applied Analysis & Computation, 8 (2018), pp. 1369–1384.
- [8] F. GÜRBÜZ, *Generalized weighted Morrey estimates for Marcinkiewicz integrals with rough kernel associated with schrödinger operator and their commutators*, Chinese Annals of Mathematics, Series B, 41 (2020), pp. 77–98.
- [9] F. GÜRBÜZ, *On the behaviors of rough multilinear fractional integral and multi-sublinear fractional maximal operators both on product L_p and weighted L_p spaces*, International Journal of Nonlinear Sciences and Numerical Simulation, 21 (2020), pp. 715–726.
- [10] F. GÜRBÜZ, *A note concerning Marcinkiewicz integral with rough kernel*, Infinite Dimensional Analysis, Quantum Probability and Related Topics, 24 (2021), p. 2150005 (14 pages).
- [11] G. JAMES, D. WITTEN, T. HASTIE, AND R. TIBSHIRANI, *Bias-variance trade-off for K -fold cross-validation. an introd. to stat. learn.-with appl. r*, 2013.
- [12] M. C. KENNEDY AND A. O'HAGAN, *Bayesian calibration of computer models*, Journal of the Royal Statistical Society: Series B (Statistical Methodology), 63 (2001), pp. 425–464.
- [13] M. KUHN, *A short introduction to the caret package*, R Found Stat Comput, 1 (2015).
- [14] J. S. PARK, *Tuning complex computer codes to data and optimal designs*, PhD, (1991).
- [15] M. PLUMLEE, *Bayesian calibration of inexact computer models*, Journal of the American Statistical Association, 112 (2017), pp. 1274–1285.
- [16] M. J. POWELL, *The newuoa software for unconstrained optimization without derivatives*, in Large-scale nonlinear optimization, Springer, 2006, pp. 255–297.
- [17] T. J. SANTNER, B. J. WILLIAMS, AND W. I. NOTZ, *The Design and Analysis of Computer Experiments*, Springer Science & Business Media, 2013.
- [18] B. SCHÖLKOPF, R. HERBRICH, AND A. J. SMOLA, *A generalized representer theorem*, in International Conference on Computational Learning Theory, Springer, 2001, pp. 416–426.
- [19] K. SOETAERT, *rootsolve: Nonlinear root finding, equilibrium and steady-state analysis of ordinary differential equations*, R package version, 1 (2009).
- [20] M. L. STEIN, *Interpolation of Spatial Data: Some Theory for Kriging*, Springer Science & Business Media, 1999.
- [21] J. STOER AND R. BULIRSCH, *Introduction to numerical analysis*, vol. 12, Springer Science & Business Media, 2013.
- [22] C. J. STONE, *Optimal global rates of convergence for nonparametric regression*, The annals of statistics, (1982), pp. 1040–1053.
- [23] E.-G. TALBI, *Metaheuristics: from design to implementation*, vol. 74, John Wiley & Sons, 2009.
- [24] R. TUO, *Adjustments to computer models via projected kernel calibration*, SIAM/ASA Journal on Uncertainty Quantification, 7 (2019), pp. 553–578.
- [25] R. TUO, Y. WANG, AND C. F. JEFF WU, *On the improved rates of convergence for Mat\`ern-type kernel ridge regression with application to calibration of computer models*, SIAM/ASA Journal on Uncertainty Quantification, 8 (2020), pp. 1522–1547.
- [26] R. TUO AND C. F. J. WU, *Efficient calibration for imperfect computer models*, The Annals of Statistics, 43 (2015), pp. 2331–2352.
- [27] R. TUO AND C. F. J. WU, *A theoretical framework for calibration in computer models: parametrization, estimation and convergence properties*, SIAM/ASA Journal on Uncertainty Quantification, 4 (2016), pp. 767–795.
- [28] S. A. VAN DE GEER, *Empirical Processes in M -estimation*, vol. 6, Cambridge university press, 2000.
- [29] G. WAHBA, *Spline Models for Observational Data*, vol. 59, Siam, 1990.
- [30] Y. WANG, X. YUE, R. TUO, J. H. HUNT, AND J. SHI, *Effective model calibration via sensible variable identification and adjustment, with application to composite fuselage simulation*, Annals of Applied Statistics, 14 (2020), pp. 1759–1776.
- [31] H. WENDLAND, *Scattered Data Approximation*, vol. 17, Cambridge university press, 2004.
- [32] R. K. WONG, C. B. STORLIE, AND T. LEE, *A frequentist approach to computer model calibration*, Journal of the Royal Statistical Society: Series B (Statistical Methodology), 79 (2017), pp. 635–648.
- [33] F. XIE AND Y. XU, *Bayesian projected calibration of computer models*, Journal of the American Statistical Association, (2020), pp. 1–18.

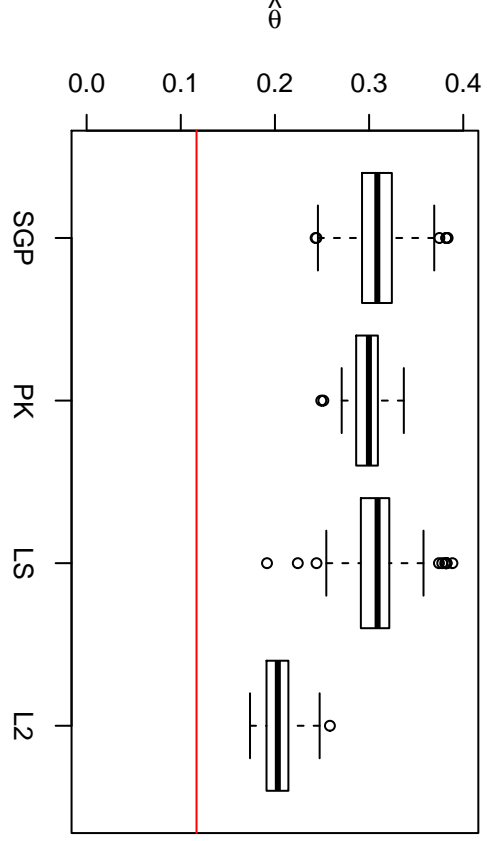
-
- [34] S. XIONG, P. Z. QIAN, AND C. J. WU, *Sequential design and analysis of high-accuracy and low-accuracy computer codes*, *Technometrics*, 55 (2013), pp. 37–46.



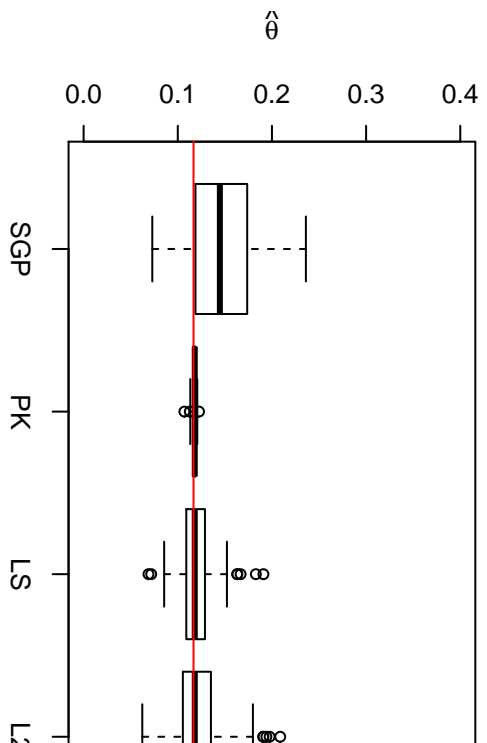
n=50



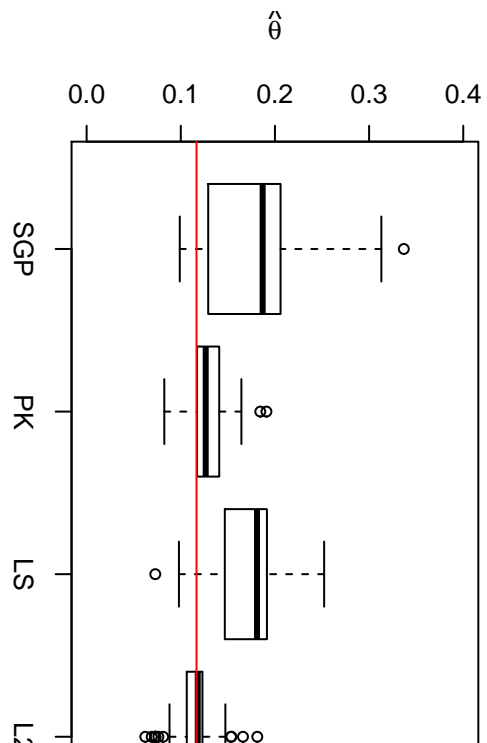
$n=50$



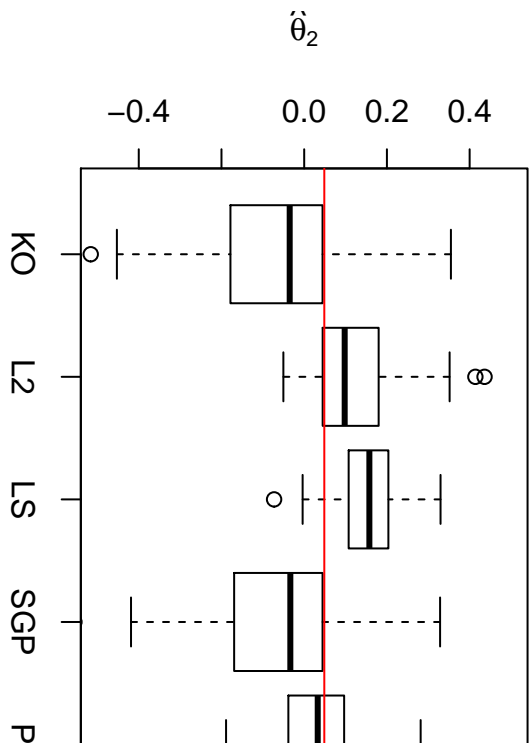
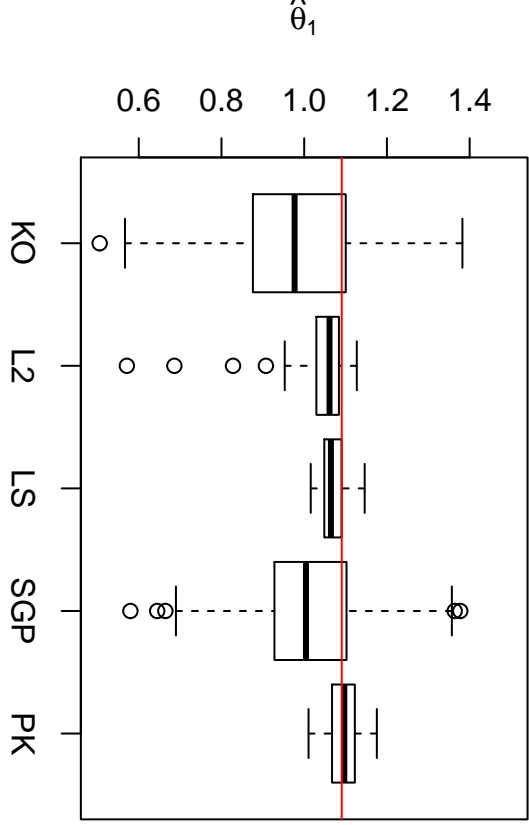
$n=6$

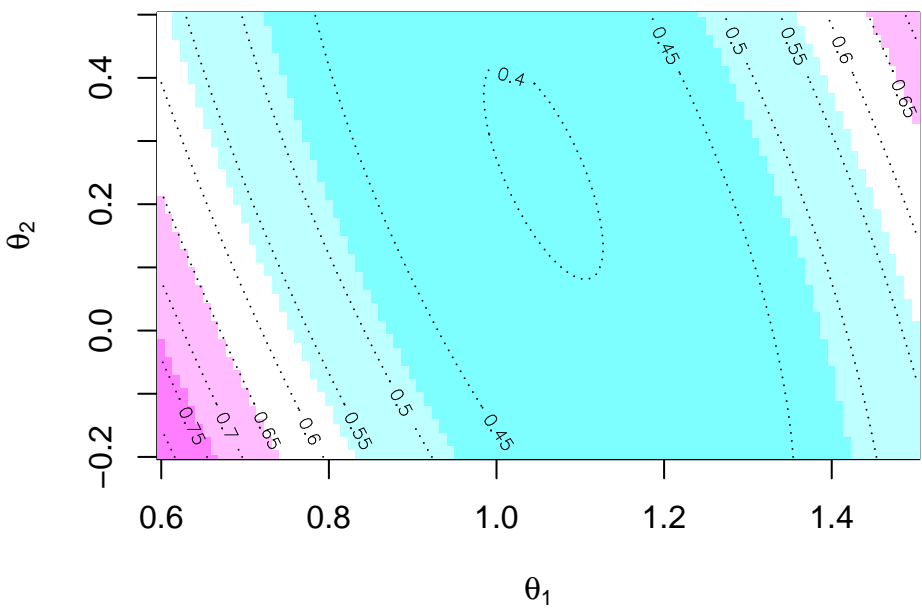


$n=100$

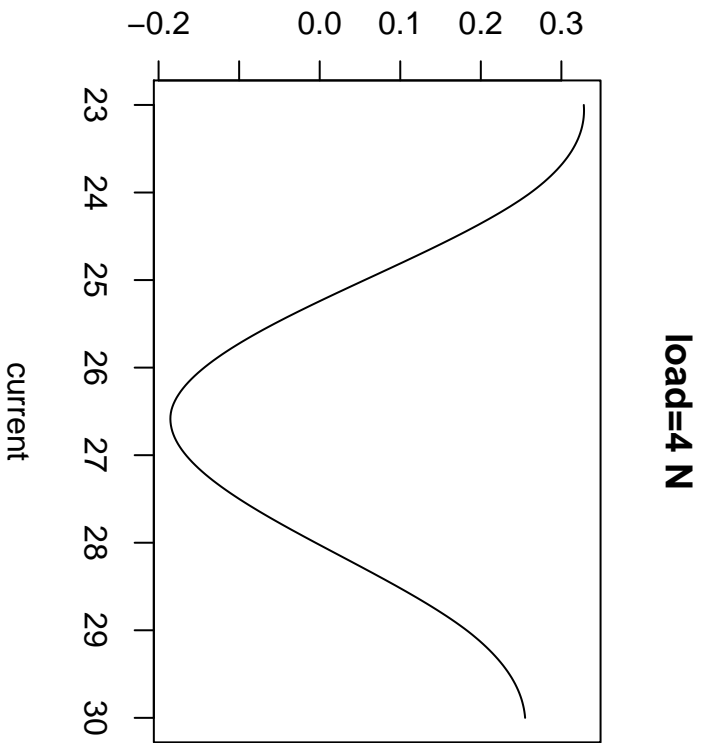


$n=20$

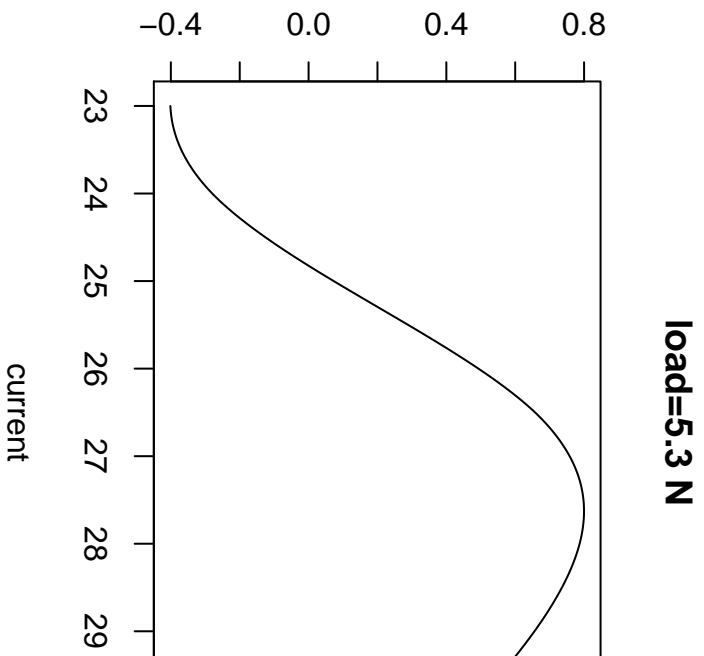


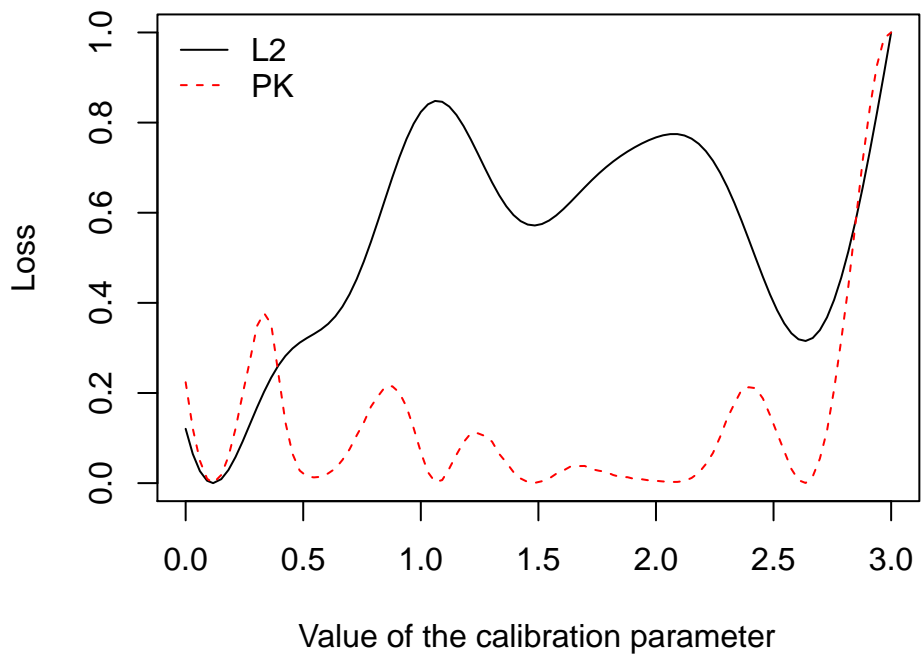


Estimation of the discrepancy function

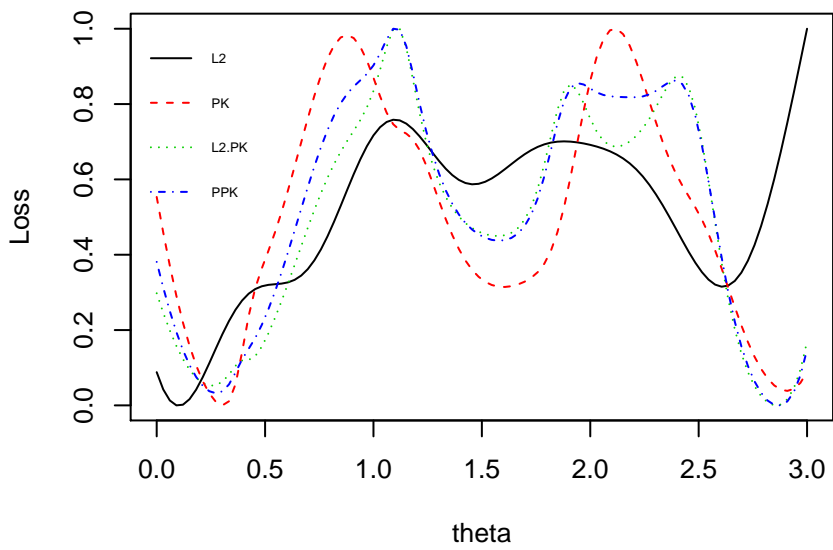


Estimation of the discrepancy function

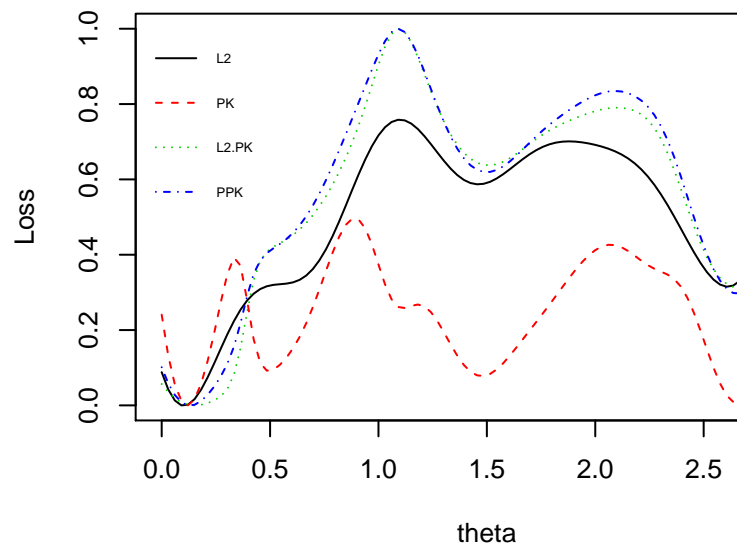




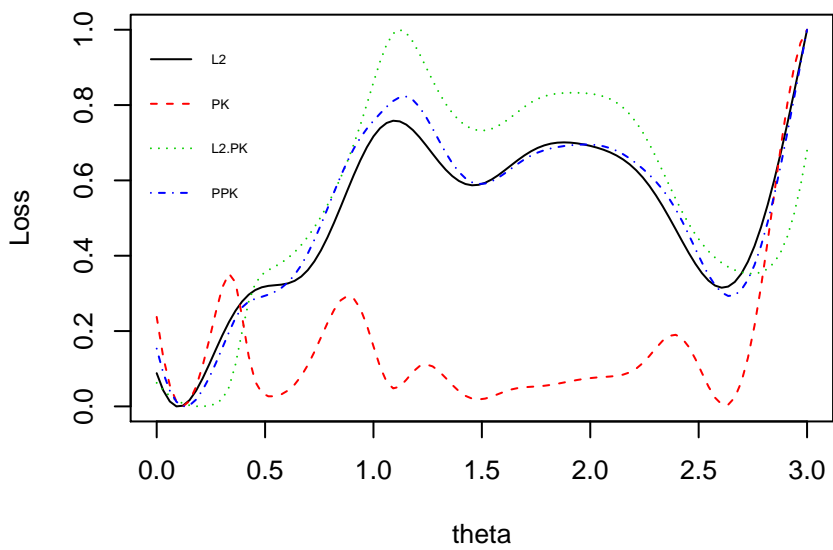
n=6



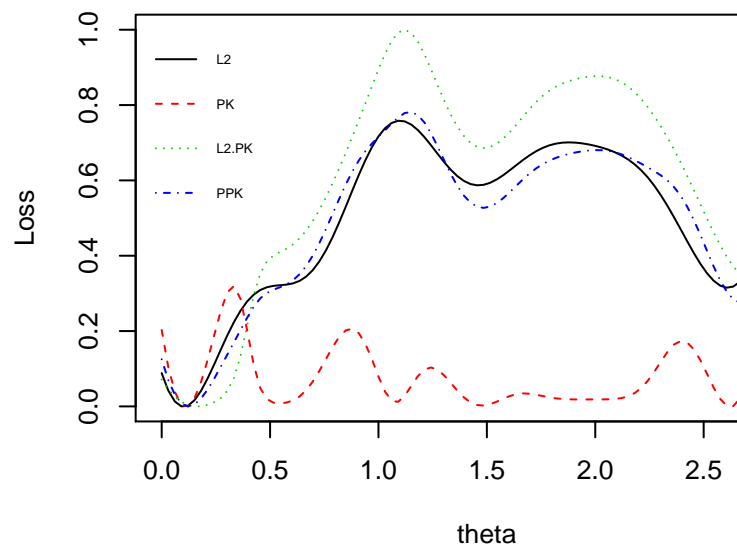
n=20



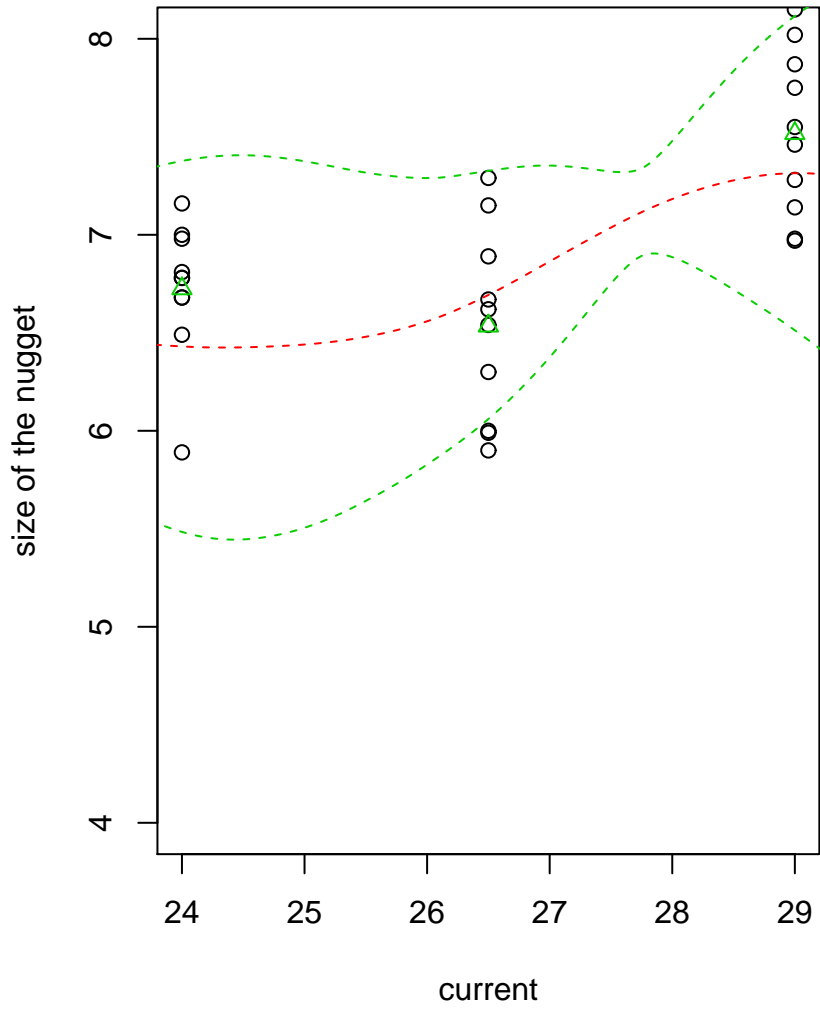
n=50



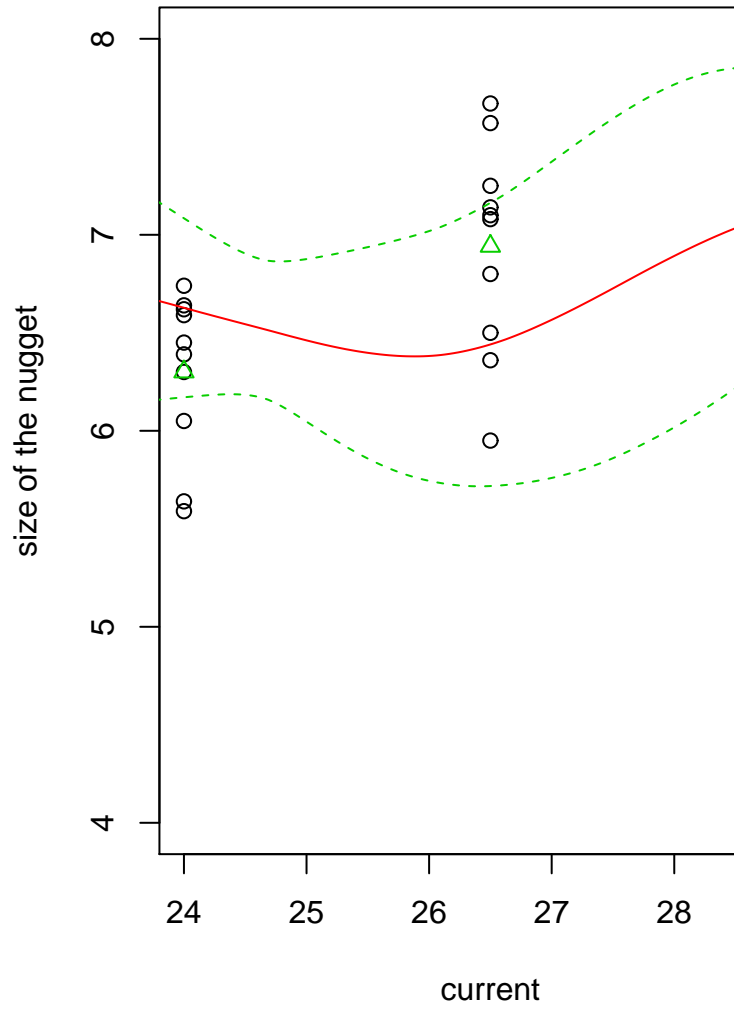
n=100



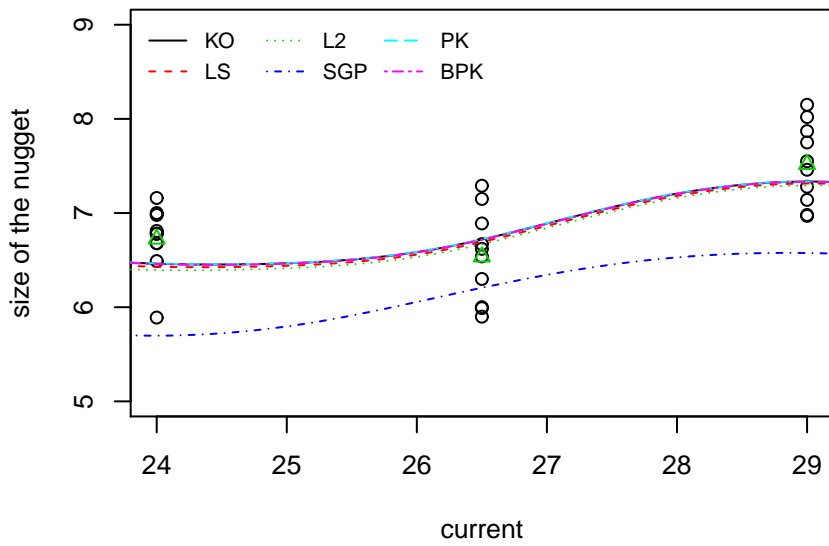
Load=4 N



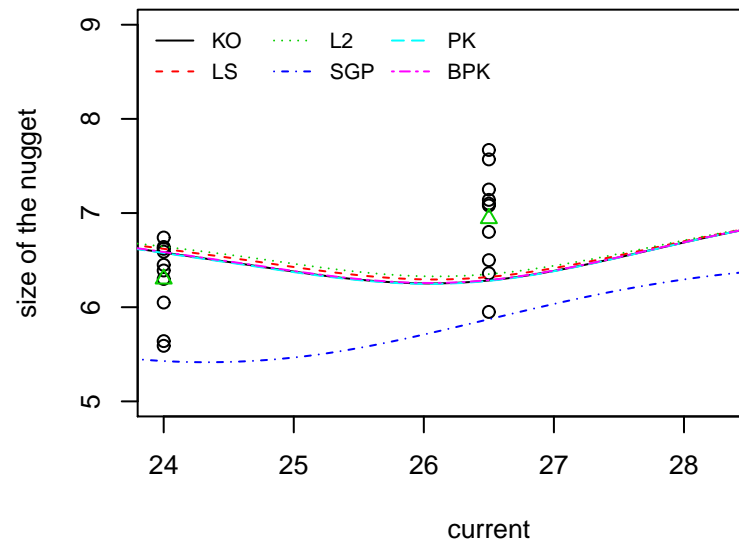
Load=5.3 N



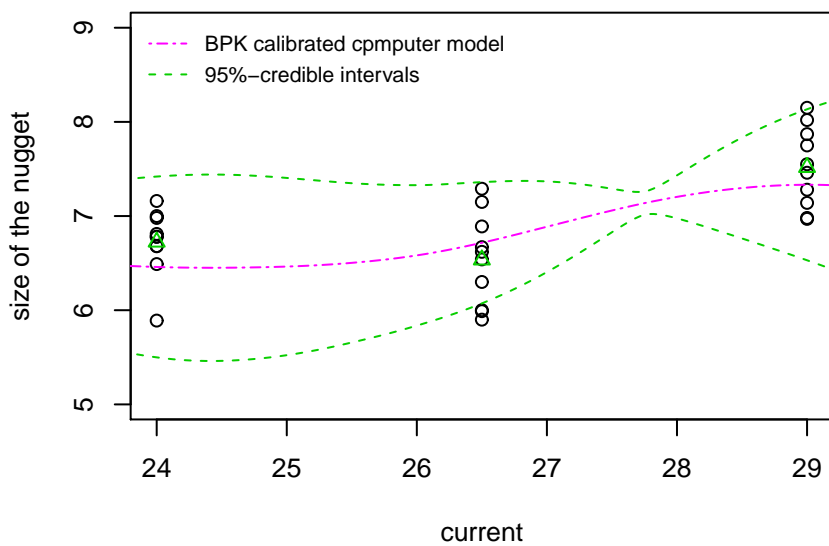
Load=4 N



Load=5.3 N



Load=4 N



Load=5.3 N

